



Investigating the potential of Ra-223 to combat Staphylococcus aureus in periprosthetic joint infections.

Stanislav Dimitrov Ivanov

Investigating the potential of Ra-223 to combat Staphylococcus aureus in periprosthetic joint infections.

by

Stanislav Dimitrov Ivanov

to obtain the degree of Master of Science

at the Delft University of Technology,

to be defended publicly on Thursday January 30, 2025 at 15:00 PM.

Student number: 5631955

Thesis committee: Dr. ir. R. M. de Kruijff, TU Delft, supervisor
Dr. Peter-Leon Hagedoorn, TU Delft
Dr. ir. I. Apachitei, TU Delft

An electronic version of this thesis is available at <http://repository.tudelft.nl/>.

Abstract

Periprosthetic joint infections by antibiotic-resistant biofilm-forming pathogenic bacteria such as *Staphylococcus aureus* are a growing concern in the field of arthroplasty. They are difficult to treat and can lead to implant revision surgery, health complications, and in some cases death. An established method in clinical practice for delivering antibiotics directly to the site of surgery is the use of antibiotic-loaded polymethyl methacrylate (PMMA), a synthetic polymer used to integrate joint implants into bone tissue. With rising rates of antibiotic resistance, researchers are looking for alternative treatments for bacterial infections and one of the possible candidates is targeted alpha therapy (TAT). Ra-223 is one such alpha emitter which is already being used in a clinical setting under the name Xofigo® to treat cancer. With the ability of PMMA to be loaded with pharmaceuticals, it may be worthwhile to investigate whether radioisotopes such as Ra-223 can also be loaded and released from the polymer. In this thesis, the potential use of PMMA as a radioisotope delivery vehicle is investigated, as well as the bactericidal capacity of Ra-223 against *S. aureus* are investigated.

To achieve this, PMMA was loaded separately with two different radioisotopes, Ga-68 and Ra-223. The loading was done with and without the presence of a chelator. The release of the isotopes from PMMA was measured over time. Growth of *S. aureus* cultures was measured under different activities of Ra-223 and growth curves were constructed. The uptake of Ra-223 by the bacteria was also measured.

A minimum of 50% Ga-68 was found to be released when freely added to PMMA. This was due to the insolubility of the Ga-68 eluate in PMMA, causing the isotope to be concentrated in a single spot. However, the addition of a chelator significantly dampened the release to maximum of 3%, since Ga-68 was homogeneously dispersed throughout the PMMA volume. Ra-223 was shown to have a similar release when added freely to PMMA (47%), but the chelator used was shown not to extract any Ra-223 to the PMMA and therefore no release was observed. There was no measurable bactericidal effect of Ra-223 on *S. aureus* for the activities used in the experiments. It was found that $8 \pm 5\%$ of the total amount of Ra-223 was taken up by the bacteria after 18 h of incubation.

Although PMMA seems to exhibit some radioisotope release, further experiments need to be carried out to determine if these amounts can evoke a bactericidal effect. The percentage of Ra-223 taken up by *S. aureus* shows that the isotope has some promise as a potential bactericide against it, but experiments with higher activities need to be carried out. Furthermore, future experiments are needed to determine the internalization of Ra-223 by *S. aureus*.

Contents

Abstract	i
1 Introduction	1
1.1 Periprosthetic joint infection	1
1.2 Polymethyl methacrylate	2
1.3 Staphylococcus aureus and its role in PJIs	3
1.4 Biofilm formation	3
1.5 Antibiotic resistance	5
1.6 Interaction of radiation and biological tissue	5
1.7 Translating TAT from cancer to infection treatment	7
1.8 Purpose of the research	7
2 Methodology	8
2.1 Materials	8
2.2 PMMA Mixing	8
2.2.1 Handling and storage	8
2.2.2 Producing a reproducible geometry	8
2.3 PMMA experiments	9
2.3.1 Effect of powder to liquid ratio	9
2.3.2 Contact time dependency	9
2.3.3 Ga-68 solubility in MMA	9
2.3.4 Ga-BPHA solubility in MMA	9
2.3.5 Ga-BPHA release	10
2.3.6 Ra-223 release	10
2.4 Bacterial culturing	10
2.4.1 Preparation of culture media	10
2.4.2 Preparation of <i>S. aureus</i> plate cultures	10
2.4.3 Preparation of liquid <i>S. aureus</i> cultures	11
2.5 Bacterial growth and uptake	11
2.5.1 Establishing a base line	11
2.5.2 Choice of cover for the well plate	11
2.5.3 Cross contamination	11
2.5.4 Growth curve experiments	12
2.5.5 Radium uptake	12
3 Results and Discussion	13
3.1 Release of radioactive isotopes from PMMA	13
3.1.1 Reproducible geometry	13
3.1.2 Powder to liquid ratio dependency	13
3.1.3 Release dependency on contact time	14
3.1.4 Solubility of Ga-68	15
3.1.5 ⁶⁸ Ga-BPHA contact time	16
3.1.6 Ra-223 release from PMMA	17
3.2 Growth of <i>S. aureus</i> in the presence of Ra-223	19
3.2.1 Establishing a baseline and choosing a suitable well plate cover	19
3.2.2 Growth curve experiments	21
3.2.3 Uptake of Ra-223 by <i>S. aureus</i>	24
4 Conclusions and recommendations	25
4.1 Conclusions	25

4.2 Recommendations 26

References **27**

A Appendix A **31**

1

Introduction

Thanks to modern medicine, humans live longer on average than ever before. Although this is a positive outcome, increased lifespan carries an inherent risk of age-related diseases. This ever-increasing problem calls for the development of new treatments and longer-lasting medical devices and, in particular, implants. The global market for medical devices was estimated at 8 billion euros in 2017, with an annual growth rate of 10% [1]. Cardiovascular implants are a substantial part of this market, driven by increasing cases of cardiovascular disease, with more than 1 million cardiovascular stents implanted annually in the United States and another million in Europe [1]. Estimates also show that 90% of the population over the age of 40 develops some type of degenerative joint disease that requires surgical intervention. From 1990 to 2000 the number of total hip replacement operations increased by 33% and by 2030 it is expected to grow to almost triple that amount [2].

Given the increasing prevalence of medical implant use, it is essential to address the associated challenges and complications. The primary modes of implant failure can be either mechanical, material-based and biological issues. Mechanical failures are commonly associated with general wear and tear, especially in weight-bearing implants like those used in orthopedics. Repeated stress and mechanical load over time can degrade materials, leading to fractures or loss of structural integrity. For example, fatigue-induced cracks can propagate under cyclic loading, ultimately resulting in implant failure. This is particularly relevant in joint replacements where the implant experiences continuous movement and load [3].

Material-based issues, including corrosion, wear debris, and bio-compatibility, contribute significantly to implant failure rates. Metal implants are susceptible to corrosion in the body's biological environment, where saline and acidic conditions can degrade metal surfaces, releasing ions that may cause local tissue reactions. For example, metallic wear in titanium alloy hip replacements has been found to cause adverse biological responses due to the accumulation of wear particles. In cases where non-metallic components are used, such as polymers in joint replacements, issues like degradation and loss of mechanical properties over time are noted, impacting the implant's durability and performance. [3].

The third type of failure which will also be the focus of this thesis has a biological origin. Biological factors, such as immune response and infection, also play a crucial role in implant failure. The body's immune system can recognize the implant as foreign, leading to inflammation or fibrous encapsulation that can affect implant integration with surrounding tissues. Infections, especially those involving biofilm-forming bacteria like *Staphylococcus aureus*, complicate this further, as they are difficult to treat and often lead to implant removal. Infections are particularly problematic in long-term implants, such as orthopedic implants, where deep-seated infections can require extensive surgical intervention [3].

1.1. Periprosthetic joint infection

Periprosthetic joint infection or PJI is one of the most challenging complications that arise from joint replacement surgery, particularly knee and hip replacement [4]. PJIs can often cause osteomyelitis and damage the implant and surrounding tissues [5]. The two leading and far the most common bac-

terial strains are *Staphylococcus aureus* and *Staphylococcus epidermidis*, the origin of which can be introduction through the surgical process or from temporary bacteraemia [5]. Sources report incidence rates for total hip arthroplasties (THA) and total knee arthroplasties (TKA) due to PJI between 2% and 2.4%. These numbers are expected to increase in the future [6]. For revision surgery, the incidence rate was estimated at 3.2% to 5.6% [7]. In the case of late PJI, that is, when the infection occurs more than 2 years after surgery, the reported incidence rate is 1.41% for TKA and 0.92% for THA. The incidence of late PJI was also observed to increase in recent years [8]. Although PJIs contribute only a small percentage of arthroplasty complications, they are responsible for 15% of all total hip revision surgeries and 25% of total knee revision surgeries [9]. This means that not only do PJIs cause harm directly to patients, but there is also a growing economic burden associated with them, as the annual cost of infected revisions in US hospitals was projected to reach \$1.85 billion by 2030 [9].

1.2. Polymethyl methacrylate

A clinically proven substance used to prevent PJI is polymethyl methacrylate (PMMA), also known as bone cement. PMMA, an acrylic resin, is widely considered the gold standard for the prevention of initial infection in orthopedic implants, particularly by using gentamicin [10]. PMMA was discovered in the early 1930s but did not see biomedical use until 1949 when it was first used to construct the first intraocular lens at St Thomas's Hospital in London [11]. Since then, PMMA has seen extensive use in the construction of orthopedic implants due to its excellent biocompatibility and its ability to resist wear and tear and infection [12].

PMMA is composed of two parts, a polymer powder and a monomer liquid (methymethacrylate), which are mixed in a typical 2:1 ratio [13]. When mixed, an exothermic reaction takes place with peak temperatures of 56° in vivo. The resulting polymer is a workable dough that can be molded until it hardens after 10 to 20 minutes, depending on the type of PMMA [13].

Although PMMA sees application in many fields, its relative uses for this thesis are those concerning the biomedical field, namely arthroplasty, vertebroplasty and drug delivery [12]. In arthroplasty and vertebroplasty, it serves two main functions, implant stabilization and bone filling, which is the original purpose of the material [13]. Cementless TKA and THA have been shown to be inferior to their cemented counterparts in terms of implant stability, fixation, and long-term survival. This is because cemented components are fixed immediately once PMMA sets, unlike cementless arthroplasties where the implant must integrate into bone tissue which can last months [14]. It is important to mention that use of PMMA in arthroplasty can have side effects, one of the most severe of which is bone cement implantation syndrome (BCIS). Although extremely rare and still poorly understood, current literature points to BCIS stemming from fragments of PMMA that enter the bloodstream during arthroplasty or thereafter. This can cause hypoxia and even cardiovascular collapse [15]. A healthy circulatory system can typically recover, but in certain cases it can result in the death of the patient [14] [15].

As one of the leading causes of TKA and THA revision is infection, PMMA has also been actively used as an antibiotic delivery vehicle in recent decades [13]. Antibiotic-loaded bone cement can be used to treat arthroplasty infections, osteomyelitis, and open fractures with bone defects [13]. There are two variants for the mixing of antibiotics in PMMA, either the cement comes premixed in the package at various doses or it can be mixed manually by the surgeon [16]. The choice of antibiotic is also crucial; the main three being gentamicin, tobramycin, and vancomycin in the case of MRSA [13]. Most premixed cements come with gentamicin due to its wide spectrum and reliable thermal stability [13] [16]. The dose and type of antibiotic are governed by the intended use of the implant being cemented. For primary arthroplasties, a low dose of less than 2 g per 40g pack is recommended as a prophylactic measure against the expected infection [16], although premixed cements commonly come with a dose of 1 g per 40g pack [13]. With revision surgeries, infection rates are higher and therefore recommended doses are also higher at 6 to 8 g [16]. Higher concentrations of antibiotics can reduce the mechanical strength of cement by as much as 40%. Therefore, a concentration of at most 5% is recommended to maintain the structural integrity of the material [14, 16].

In addition to antibiotics, PMMA can be loaded with other substances. For example, quaternized bone cement loaded with chitosan has been shown to inhibit biofilm formation in *S. epidermidis* and *S. aureus* [17]. Furthermore, isotope-loaded PMMA has also been investigated as an alternative form of

brachytherapy [18],[19]. This highlights the potential use of PMMA as a radiopharmaceutical delivery vehicle.

1.3. Staphylococcus aureus and its role in PJIs

As mentioned in Section 1.1, the two main culprits behind PJIs are *S. aureus* and *S. epidermidis*, with the focus of this thesis being on the former. *Staphylococcus aureus*, discovered in the 1880s, is a spherically shaped Gram-positive bacterium typically found in the upper respiratory tract and skin. It is estimated that around 50% of the human population carries *S. aureus* with 20% being continuous carriers [20]. Although usually a component of the human microbiome, it has the ability to become pathogenic. In fact, before the invention of penicillin, the mortality rate of an *S. aureus* infection was 80%. Just two decades after the invention of penicillin in 1940, 80% of *S. aureus* strains were resistant to it [21]. Two years after methicillin was invented in 1961, through the acquisition of the gene *mecA*, Methicillin-resistant *S. aureus* (MRSA) was born [11].

Naturally, this pathogenesis also extends to medical implants. All surgical implants carry the inherent risk of being accompanied by a nosocomial infection. These foreign objects cause inflammation around the surgical site, decreased immune response, and are often made from materials suitable for bacterial adhesion and subsequent colonization [22]. Due to the fact that *S. aureus* is present on the skin of patients, open surgery such as TKA or THA is an opportunity for these skin-dwelling bacteria to enter the surgery site and possibly colonize the biomaterial [23]. At this point, the so-called "race for the surface" begins between bacterial and host cells. The outcome of this "race" determines who will attach and colonize the material first [24]. In the event that bacteria reach the surface first, they attach and begin to form colonies. At this point, the infection that occurs can still be treated with the right antibiotics, but this becomes increasingly difficult if the infection becomes chronic or the pathogen starts forming a biofilm [24],[25]. Indeed, *S. aureus* is one such biofilm-forming pathogen.

1.4. Biofilm formation

The idea that bacteria do not exist only in the planktonic state but can also form more complex structures has existed ever since the invention of the microscope. However, the term biofilm infection first came about in the medical field around the 1980s[26]. Biofilms account for more than 80% of microbial infections in the body [23]. There are many definitions of bacterial biofilms, but in the most general sense, they are a structured group of bacteria that are encased in a self-made extracellular matrix [27]. The microorganisms that make up a biofilm can differ greatly from their planktonic counterparts. This is because proteins expressed in both states of the microbe result in a different phenotype [5]. Not only do biofilm cells possess a different phenotype, but they are also highly differentiated, with each bacterium performing a different function within the biomass.

The current consensus in scientific literature is that the cycle of a biofilm consists of four distinct steps (see Fig. 1.1): Attachment, Growth, Maturation and Detachment [28].

Attachment

In this initial step, free floating planktonic bacteria adhere to the surface of an implant via polarity, London-van der Waals forces, and hydrophobic interactions [29]. This step is sometimes further differentiated into a reversible and an irreversible attachment. The former refers to the fact that when bacteria have not yet differentiated, adhesion to the surface is still weak. Once the population grows, the bonds between the bacteria and the surface, as well as between the bacteria and the bacteria, become stronger, and the attachment becomes irreversible.

Growth

After the bacteria are firmly attached to the surface, multiplication begins. In the particular case of *Staphylococci*, the antigen called polysaccharide intercellular adhesin, or PIA, leads to adhesion and biofilm accumulation [30]. In this step, quorum sensing (QS) plays a very important role in organizing and regulating bacterial cells within the microcolony that forms [23]. Quorum sensing is essentially cell-to-cell communication for bacteria and is most effective in dense populations such as biofilm. Through this process, bacterial populations can, depending on density, communicate which genes are beneficial to express [31]. In *S. aureus* QS is governed by the *agr* locus, which consists of four genes: *agrA*, *agrD*, *agrC* and *agrD* [23].

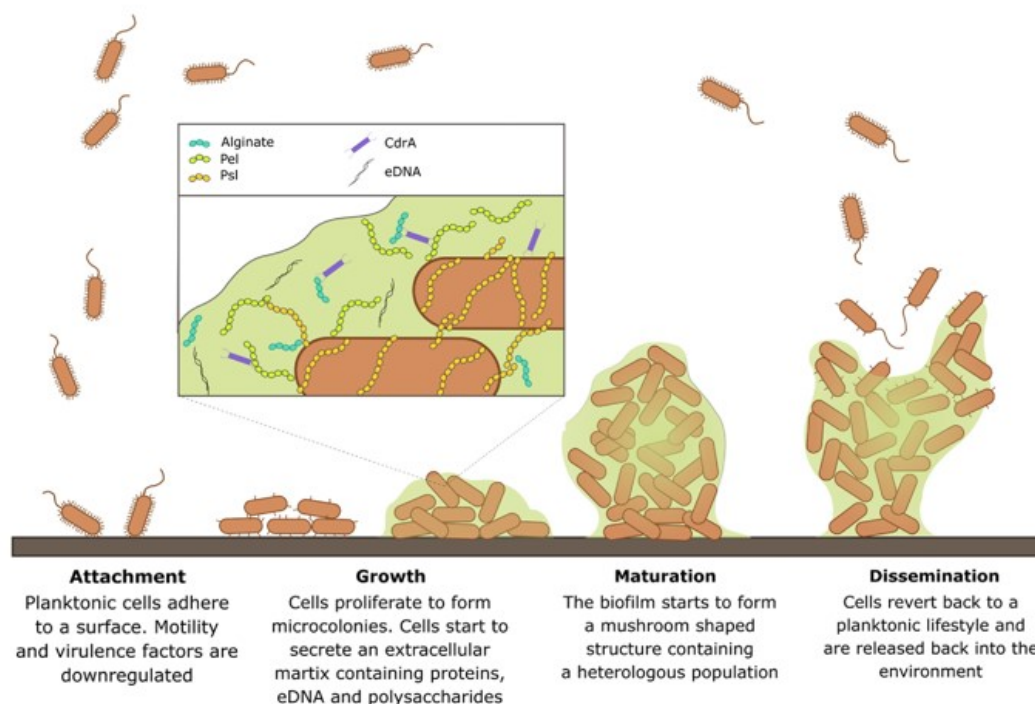


Figure 1.1: The four steps of biofilm lifecycle which are from left to right: Attachment, Growth, Maturation and Detachment. [28].

As the number of bacterial cells grows, multiple cell layers are formed (see Fig. 1.2) and this mass of cells begins to produce extracellular polysaccharide substances (EPS) [23]. The deepest layer, called the conditioning film, is what facilitates the adhesion of the biofilm to the biomaterial surface. On top of it lies the base film, which contains the bulk of biomass, and the outer layer, called the surface film, is where planktonic bacteria are being continuously released to spread and colonize other sites. [5].

EPSs are an insoluble slimy substance that encases millions of neighboring cells and forms a firm organized matrix [23]. EPS offer a multitude of benefits for the encapsulated colonies. First, they strongly aid in the adhesion of bacteria to the biomaterial surface. Second, they disseminate and spread nutrients important for the survival and growth of colonies. And finally, they offer a protective barrier against host defenses and bactericidal substances [23].

Maturation

Once enough biomass has accumulated inside the biofilm, the structure starts to resemble a tower. The high density of cells allows QS to flourish. This is the process through which bacteria encased in a biofilm can diverge phenotypically from planktonic bacteria. For example, biofilm bacteria may have an over-expression of efflux pumps, which essentially allows them to remove antibiotics faster from the cell [31]. In *S. aureus* specifically, the agr QS system is responsible for the regulation of the virulence factor. In addition, defensive factors to avoid host immune response and promote bacterial internalization and host cell apoptosis are also up-regulated [23],[5]. Another component is closely related to biofilm formation and stability in *S. aureus*, namely extracellular DNA (eDNA). eDNA improves the structure of the biofilm and can help facilitate horizontal gene transfer between cells, enhancing antibacterial and antibiotic resistance within the biofilm [32],[5].

Detachment

Once critical mass is achieved, bacteria near the surface of the biofilm can escape and return to their planktonic state. Herein lies the danger of biofilm infections. Biofilms can act as a persistent source of virulent planktonic bacteria that can spread around the body and repeat the process [23].

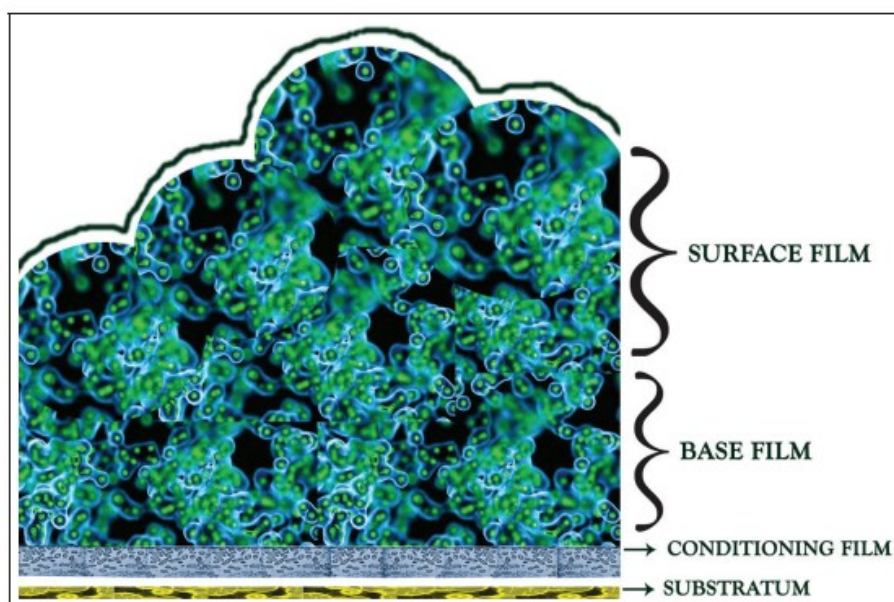


Figure 1.2: The three main layers comprising the structure of a biofilm [23].

1.5. Antibiotic resistance

Biofilms acting as reservoirs of infection are problematic because not only are planktonic bacteria increasingly antibiotic resistant, but the biofilm itself is oftentimes inherently also antibiotic resistant.

There are multiple factors associated with this induced antibiotic resistance. In general sense, the physical barrier that the biofilm provides serves to slow down the diffusion of antibiotic and antimicrobial substances [31]. This results in substances being unable to reach the deep-situated cells inside the macrocolony.

As mentioned in the previous section, eDNA and QS promote horizontal gene transfer and communication between cells. This results in the proliferation of genes related to antibiotic resistance. Furthermore, QS is also responsible for high cellular differentiation within the biofilm. Planktonic bacteria and bacteria within the biofilm are phenotypically different and exist in different stages of development, making them resistant to a wide spectrum of antibiotics [31]. Antibiotics are effective mainly against actively dividing cells; however, deep within the biofilm there exist so-called persister cells, which are highly tolerant to antibiotics [33].

1.6. Interaction of radiation and biological tissue

Because bacteria inside the biofilm are resistant not only to antibiotics but also to a wide range of antimicrobial agents, it stands to reason that efforts should focus on prevention of biofilm formation rather than treatment. There are already a multitude of prevention and treatment strategies under investigation, from antimicrobial coatings on implants to biomaterial surface modifications for prevention to bacteriophage therapy and photodynamic therapy for treatment [34],[35],[36],[37],[38].

Another relatively unexplored prevention and treatment strategy is the use of radiation to target and treat infections. The interaction between biological matter and radiation has already been extensively studied in the fields of radiology and medical physics. An important concept in radiobiology is linear energy transfer (LET), which describes the energy (E) transferred per unit length (l) of the track of a charged particle [39],

$$LET = \frac{dE}{dl} \left[\frac{keV}{\mu m} \right] \quad (1.1)$$

Among radiation types, alpha particles generally have one of the highest LETs up to $100 \text{ keV}/\mu\text{m}$ [39].

Another important quantity in the radiation-tissue interaction is the relative biological effectiveness (RBE). Formally, RBE is measured as the dose ratio of 250 kV X-rays (D_{250}) and another type of radiation D_r that causes the same biological damage:

$$RBE = \frac{D_{250}}{D_r} \quad (1.2)$$

In general, the dose of 250 kV X-rays can be substituted for any reference absorbed dose [39].

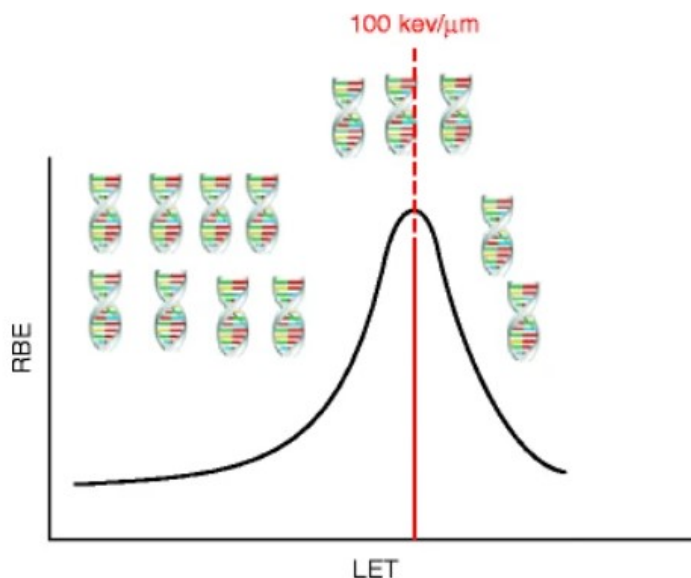


Figure 1.3: A simplified illustration of the overkill effect. Increasing LET leads to increasing RBE up to the point where LET reaches $100 \text{ keV}/\mu\text{m}$. After this point the ionization density is higher than what is required to kill a cell so the radiation kills less cells per absorbed dose [40].

For mammalian cells, RBE increases proportionally to the increase of LET to a point (around $100 \text{ keV}/\mu\text{m}$, after which it begins to decrease again (see Fig. 1.3) [39], [40]. The decrease in RBE despite increasing LET is called the overkill effect and indicates that there is an optimal amount of ionizing effects necessary to kill cells [39].

Radiation types vary in their LET, which plays a crucial role in determining the extent and complexity of the damage caused. Low LET radiation, such as X-rays, tends to cause more dispersed ionization events, resulting in simpler DNA damage like single-strand breaks, which cells can often repair effectively. However, high LET radiation, such as alpha particles, produces dense ionization clusters that lead to more complex and severe damage, including double strand breaks in DNA. These breaks are particularly lethal because they are difficult for the cell to repair, often leading to cell death, apoptosis, or long-term genetic mutations[41].

In addition to direct damage to cellular DNA, radiation can cause indirect damage by interacting with the substrate around the targeted tissue to create what are known as reactive oxygen species (ROS). These ROS can in turn react with target cells and accumulate additional damage [42].

As already stated, alpha particles have highly favorable qualities if the goal is to target and kill cells. As such, targeted alpha therapy (TAT) has been a rapidly evolving subfield of radionuclide therapy [43]. In the context of cancer therapy, TAT is useful with its short range of 50 to $100 \mu\text{m}$ and its mean LET of $100 \text{ keV}/\mu\text{m}$, which makes it ideal for targeting small volumes of cancerous cells without accumulating a lot of energy in the surrounding healthy tissue [44]. Alpha particles have also been shown to be effective in hypoxic environments unlike low LET radiation and have a very high RBE of 3 to 8 [44]. When paired with the right transport molecule, alpha particles can be delivered to the desired location while mostly sparing other sites [43], [44], [45].

It is also important to mention some of the drawbacks of TAT. To begin with, the research, evaluation and development of a radiopharmaceutical is a long and difficult process [45]. In addition, daughters of alpha emitters can escape the tumor site and travel to surrounding healthy tissue, thus increasing toxicity for patients [46]. This is known as the recoil problem. However, by far the biggest problem associated with alpha therapy is the difficulties in sourcing and producing alpha radionuclides [45, 46].

1.7. Translating TAT from cancer to infection treatment

Despite its problems, TAT remains a promising field of research. This research is now beginning to expand beyond the realm of cancer treatment into fields such as viral, fungal, and even bacterial infections [47]. Given the considerable advances in radiotherapy and, in particular, radioimmunotherapy (RIT) over recent decades, which have solidified their roles as effective cancer treatments, researchers are now exploring whether the targeting principles employed in these therapies could be effectively adapted for the treatment of bacterial infections [48]. Alpha and even beta radiation has already been used in in-vitro studies against *Streptococcus pneumoniae* and *Bacillus anthracis* with promising results [49],[50]. Alpha emitters showed a greater bactericidal effect than beta emitters, possibly due to the higher LET and shorter range of alpha particles [50].

The bactericidal effect of alpha and beta emitters has also been tested on *S. aureus*. Three isotopes, Bi-213, Lu-177, and Ac-225, were used to treat in vitro planktonic and biofilm MRSA. Of the three isotopes, the alpha emitting Bi-213 showed the greatest killing ability while Lu-177 a beta emitter showed no effect. Ac-225 was found to increase the metabolic activity of MRSA in both planktonic and biofilm forms. It speculated that the results for Ac-225 could be due to its longer half-life and its biofilm disrupting effect might cause a temporary increase in metabolic activity due to bacterial dispersal. The conclusion of the study was that the half-life of the alpha emitter may have an impact on its ability to kill bacteria, as Bi-213 showed a greater killing effect than Ac-225, but further investigation was necessary [51].

Alternatively, radiotracers such As-111, Tc-99m, Ga-68, C-11, and F-18, in conjunction with monoclonal antibodies (mAb) and antimicrobial peptides (AMP), are also promising candidates for the imaging and diagnosis of bacterial infections according to research [52],[53]. Another alpha emitter currently used in the clinical setting to treat castration-resistant prostate cancer bone metastases under the name Xofigo®, is radium-223 [44]. It is an alpha emitter with a half life of 11.4 days which decays to the stable Pb-207 through four alpha decays and two beta decays [54]. Radium-223 has a proven track record since 2013 for the treatment of mCRPC, and further studies have investigated its possible use in breast cancer[55]. Its multiple alpha emissions and relatively long half-life make it a suitable candidate to investigate controlled release for the purpose of infection prevention.

1.8. Purpose of the research

With the expanding literature on the use of radioimmunotherapy to tackle the problem of bacterial infection and the current developments of loading PMMA with radioisotopes, it could be viable to explore whether isotopes can be loaded onto bone cement and released locally over time.

As infection treatment is still a largely unexplored territory, the main objective of the thesis is to explore the viability of the alpha radionuclide Ra-223 as a possible antibacterial agent in the context of *S. aureus* in PJI. This can be broken down into several sub-aims of the study. First, the available literature points to PMMA as a possible vehicle of not only antibiotics but also other substances. Therefore, a purpose of the study is to explore whether and how radioactive isotopes such as Ga-68 and Ra-223 can be effectively loaded into PMMA and what their release over time is. A further objective is to test the bactericidal effect of Ra-223 against *S. aureus* based on different amounts of activity and, last, to measure the uptake of this radionuclide by bacterial cells.

2

Methodology

2.1. Materials

Product name	CAS number	Supplier
Brain Heart Infusion Agar	-	Sigma Aldrich
Brain Heart Infusion Broth	-	Sigma Aldrich
Dulbecco's Phosphate Buffered Saline	-	Biowest
Gallium-68	-	-
HCl	7647-01-0	VWR International
N-Benzoyl-N-phenylhydroxylamine, 98%	304-88-1	Thermo Scientific
PALACOS® LV	-	Heraeus Medical
Tris	77-86-1	Merck Sigma
Xofigo®(RaCl ₂)	-	GE HealthCare

2.2. PMMA Mixing

2.2.1. Handling and storage

For experiments involving PMMA the Heraeus PALACOS®LV was used. It is a low-viscosity radio-opaque bone cement that comes in two separate components of a sealed package of 40 g of powder and 20 ml of liquid (referred to as MMA hereater) containing a glass ampule. This particular brand of bone cement has a green-dyed MMA liquid resulting in a green bone cement mixture. The two components were transferred to separate plastic containers for easy use and stored in a fume hood. The MMA part of the cement was kept away from direct sunlight, as UV rays cause the MMA to polymerize, rendering it unusable for cement mixing. Another consideration was to use a plastic tube with a sealed screwcap, since MMA is highly volatile and will evaporate if stored for a prolonged period of time.

2.2.2. Producing a reproducible geometry

In a clinical setting, bone cement is typically mixed by dumping all contents of both parts inside a container and hand mixing or alternatively using a specialized tool for vacuum mixing. Thus, the recommended ratio of powder to liquid is 2:1, which was kept for the entirety of the PMMA-related experiments, unless otherwise specified. Since this procedure exhausts the entire pack of cement, for an experimental setting a new mixing procedure had to be made. Initially 2 grams of powder and 1 ml of MMA were used to test out hand mixing of small amounts of cement inside an agar plate. Smaller

volumes of mixture were also mixed into a 6-well plate.

An alternative method was attempted using a 2 ml and a 1 ml syringe as a mixing container. The tip of the syringe was sealed using parafilm and the plunger was removed. 500 mg of powder was inserted into a 2 ml syringe, after which the plunger was reinserted into the syringe and the parafilm was removed. Using a pipette, 250 μl of MMA was added to the syringe through the tip and repeated plunger motions were made to mix both parts of the cement.

This was followed by an attempt to downsize to a 1 ml syringe and 250 mg of powder. Instead of mixing with the plunger, a needle would be inserted through the tip of the syringe after adding the 125 μl liquid to mix both powders by swirling conic motion.

Since manual mixing proved to be problematic, mixing with a vortex was explored as a result. Several different containers were tried among which 50 ml and 15 ml Eppendorf tubes and 1.5 ml SafeSeal microtubes were tested with 12.5 mg and 25 mg for all three tube types.

27 mg of bone cement powder were mixed with 12.5 μl of MMA in a SafeSeal microtube on a Vortex-Genie 2 set with maximum speed and touch function. This was done by first adding the MMA to the microtube, then dumping the powder, closing the microtube and vortexing for 15 s.

2.3. PMMA experiments

Gallium-68 was eluted from a Ge-68/Ga-68 generator. Using 5 ml of 0.1 M HCl, an elution containing 7.32 MBq could be eluted from the generator, which is equivalent to 1.46 kBq/ μl . The actual value would vary since for the experiments with PMMA, only 3 ml of HCl was used to produce a more concentrated elution. The activity was also dependent on how often the generator was used for the elution, since each consecutive elution in a limited time would result in less activity. The exact activity is not relevant in the context of the release of Ga-68 from PMMA, as the released activity was measured in % of the total activity.

2.3.1. Effect of powder to liquid ratio

An initial experiment was carried out with four different ratios of powder to MMA of 1.7:1, 1.85:1, 2:1 and 2.15:1 to see if this would affect the release of gallium. 23 mg, 25 mg, 27 mg and 29 mg were mixed with 12.5 μl of MMA with 0.5 μl of Ga-68. This was done by first adding Ga-68 to MMA and then following the same procedure as described in the previous subsection. An initial measurement was done on a Perkin Elmer-Wallac Wizard 1480 3 inch Gamma Counter (hereafter referred to as the Wallac) to record the total amount of radioactivity in the mixture. The cement was left to dry for 20 min, after which 1 ml of Phosphate Buffered Saline with a pH of 7.4 was added on top of the samples. The four samples were left in contact with PBS for 20 min, after which the liquid was pipetted for measurement and new PBS was added for another 20 min. After the second batch of PBS was measured, the residual activity in the PMMA was also measured.

2.3.2. Contact time dependency

1 μl of Ga-68 was added to 12.5 μl of MMA and mixed on a vortex with 27 mg of bone cement powder. The procedure of Section 2.4.1 was repeated. After bone cement dried for 20 min, 0.5 ml of PBS was added three consecutive times for an equal amount of contact time. The initial and final activity, as well as the activity in each batch of PBS, was measured. This was done for contact times of 1, 5, 10 and 20 min.

2.3.3. Ga-68 solubility in MMA

The solubility of the eluate from the $^{68}\text{Ge}/^{68}\text{Ga}$ generator in MMA was tested by adding 5 μl of Ga-68 to 25 μl of MMA and another solution of 5 μl Ga-68 mixed with 25 μl of MilliQ was used as a control sample. From each sample, 3 equal fractions of 3 μl of the solution were pipetted out and measured on the Wallac. The initial and final activity in the samples was also measured.

2.3.4. Ga-BPHA solubility in MMA

N-benzoyl-N-phenylhydroxylamine (BPHA) was chosen for the extraction of gallium from HCl. 42.6 mg of BPHA was added to 1 ml of MMA to form a solution of 0.2M BPHA. The solution was vortexed for

1 min to ensure BPHA was dissolved. 100 μl of Ga-68 eluate was added to the solution and placed on the Vortex-Genie 2 for 10 min. 3 subsamples of 10 μl were pipetted from the upper layer of the solution and measured on the Wallac.

2.3.5. Ga-BPHA release

The experiment of Section 2.4.2 was repeated, this time with the added step of incorporating BPHA in MMA. 42.6 mg of BPHA was added to 1 ml of MMA and 100 μl of Ga-68 was added. The solution was vortexed for 10 min. The procedure then retraces the one in 2.4.2, but this time directly adding 13.5 μl of Ga-BPHA-MMA solution to a SafeSeal microtube, adding 27 mg of powder and mixing on the vortex for 30 s. After drying for 20 min, 0.5 ml of PBS was added on top of the sample for a contact time of 5 or 20 min, after which it was pipetted and a new 0.5 ml was added to the sample. The initial, final and PBS sample activities were measured on the Wallac.

2.3.6. Ra-223 release

For the Ra-223 release experiment a single contact time of 1 day was chosen due to the 11.4 day half-life of the isotope. Two separate release experiments were ran simultaneously.

In one 1 μl Xofigo®(equal to 0.69 kBq at the time of the experiment) was directly added to 12.5 μl of MMA and mixed with 27 mg of powder on a vortex. After drying for 20 min, 0.5 ml of PBS was added on top of the sample for a contact time of 1 day, after which it was pipetted and a new 0.5 ml was added to the sample. The initial, final and PBS sample activities were measured on the Wallac. In addition to measuring the activity of Ra-223, the activity of Pb-211, a daughter of the Ra-223 decay chain, was also measured.

Since Xofigo is an aqueous solution, to avoid the need for a follow-up experiment, in conjunction with the pure batch of Xofigo, another batch of PMMA was prepared by adding 49 mg of Tropolone, an organic soluble chelator, to 2 ml of MMA to make a 0.2 M solution. From this stock solution 100 μl was pipetted and 7.5 μl of Xofigo (equal to 5.18 kBq at the time of the experiment) was added to it. The mixture was vortexed for 10 min to ensure enough radioisotope was taken up by the MMA-Tropolone solution. Following this 13.5 μl of MMA was mixed with 27 mg of powder on a vortex. After drying for 20 min, 0.5 ml of PBS was added on top of the sample for a contact time of 1 day, after which it was pipetted and a new 0.5 ml was added to the sample. The initial, final and PBS sample activities were measured on the Wallac. The activity of Pb-211 was measured again each time. Subsequently, one sample from both batches of PMMA was measured on a germanium detector for comparison.

2.4. Bacterial culturing

2.4.1. Preparation of culture media

The culture mediums of choice for this project were Brain Heart Infusion Broth (BHI Broth) and Brain Heart Infusion Agar (BHI Agar). Both mediums were prepared according to the manufacturer's instructions [56], [57]. For BHI broth, 37 g of powder was mixed with 1000 ml of MilliQ, autoclaved at 121°C for 15 minutes. After being cooled, it was separated into smaller 200 ml bottles inside a biosafety cabinet for easier handling. The medium was stored in a cabinet at room temperature (21 °C). For the solid BHI agar medium, 26 g of powder was dissolved in 500 ml of MilliQ and subsequently autoclaved at 121°C for 15 minutes. After a slight cooling period, the agar was poured onto agar plates, either by simply pouring it out onto the plate or via a serological pipette. The exact amount for this step was not crucial and anywhere between 20 and 30 ml of agar per plate was sufficient to produce and maintain bacterial colonies. The plates were then allowed to solidify for 20 minutes and dried for another 20 to 30 minutes, which could be done either in the biosafety cabinet or in an incubator at 37°C. Once dry, plates were closed, sealed with parafilm, and stored in a fridge at 4°C. As the agar solidifies at room temperature, subsequent pouring of it on plates required to heat it up which could be done using a conventional microwave or autoclaving for 15 min at 121°C.

2.4.2. Preparation of *S. aureus* plate cultures

The chosen strain of *S. aureus* was RN0450 which is a methicillin-susceptible strain of the bacteria, commonly used for research purposes. Initially, bacteria taken from a stock were used to inoculate three agar plates. Subsequent plate cultures were made using bacteria from a previously inoculated

plate to ensure the availability of fresh and healthy colonies at all times. Inoculation of a new batch of agar plates was performed every two weeks. The inoculation procedure was done using the streaking method, in which an inoculation loop was used to pick out a single colony, plant it on a fresh agar plate, and using the pointy end of the loop streaking the bacteria across the agar surface. This procedure was performed inside a biosafety cabinet. The plates were then incubated in a Heraeus HeraCell incubator at 37°C for 18 hours, after which they could be sealed with parafilm and stored in a fridge at 4°C.

2.4.3. Preparation of liquid *S. aureus* cultures

Preparation of liquid cultures was done by pipetting 50 ml of BHI broth into a 250 ml glass round bottom flask, then using an inoculation loop picking out a single *S. aureus* colony from an agar plate and adding it to the liquid medium. This step was primarily accomplished by simply breaking the loop end and leaving it inside the flask. Alternatively, a toothpick could be used to remove the colony from the agar plate after which it could be simply dropped inside the liquid medium. The flask was then sealed with a double layer of aluminum foil and placed in a New Brunswick Scientific C24 Incubator Shaker at 37°C, 155 rpm for 18 h for incubation. The incubated culture was used directly after the incubation process for experimentation.

2.5. Bacterial growth and uptake

For the series of experiments involving bacterial growth and uptake of *S. aureus* ²²³RaCl₂ containing a specific activity was used at the time of receiving of 1.1 MBq / ml. 24 well-plates were deemed optimal for the amounts of bacterial culture and radioactivity used. Well plates were chosen over round bottom flasks due to the availability of a Biotek PowerWave XS plate reader equipped with incubation and shaking functionality which was used to perform OD630 measurements. Growth curves were estimated the Slogistic1 (2.1) model in Origin Pro.

$$OD630 = \frac{OD630_{max}}{1 + e^{-\mu_{max}(t-t_i)}} \quad (2.1)$$

Here, $OD630_{max}$ is the maximum OD value reached during growth, μ_{max} is the highest growth rate, and t_i is the inflection time at which is the point in time when growth starts to decrease.

2.5.1. Establishing a base line

Five wells in a 24-well plate were filled with 1.5 ml of BHI broth to which 7.5 μ l of precultured *S. aureus* was added, a dilution factor of 201x. The plate was placed in the PowerWave XS plate reader and incubated and measured for 18 h at 37°C and a low shake speed. A total of 20 measurements were performed and a base line growth curve was established.

2.5.2. Choice of cover for the well plate

Three considerations needed to be taken for this round of experiments. First, the available 24-well plates were too thick for the plate reader and had to be inserted without a lid, which meant that due to prolonged exposure to a temperature of 37°C, it was possible to release Ra-223 outside the well. Second, *S. aureus* requires oxygen to grow, which means that insulating the well plate might lead to insufficient growth of bacteria. And finally, covering the well plate with any form of material meant that the OD630 measurements could be affected. Two candidates were tested to cover the well plate; one is a standard mylar film, and the other is a Plate Sealer from Thermo Scientific. A single 24-well plate was divided into two equal parts, one covered with mylar film and the other with Plate Sealer. 1.5 ml of BHI broth was added to all wells in the well plate, to which 7.5 μ l of 7.5 μ l of pre-cultured *S. aureus* was added. The plate was incubated for 18 h at 37°C and a low-shake speed and a total of 20 measurements were performed over 18 h. No radiation was used in this experiment.

2.5.3. Cross contamination

After the appropriate choice of a cover for the well plate, a cross-contamination experiment was performed to ensure that radiation would not migrate from one well plate to neighboring well plates. A single well in the center of the plate was filled with 1.5 μ l of BHI broth. 1 μ l of RaCl₂ was added to it. The neighboring wells were filled with 1.5 ml of water, the plate was sealed with a Plate Sealer and put

in the Plate Reader for 18h at 37°C. The liquid from the wells was then pipetted and measured on the Wallac.

2.5.4. Growth curve experiments

To test the effect of Ra-223 on *S. aureus* four different activities were used. On a single well plate, four rows were filled with 1.5 ml of BHI broth and 7.5 μl of *S. aureus* pre-culture. One row was left without radium to serve as a control. To the other three rows an activity of 100 Bq, 500 Bq, and 1 kBq of Ra-223 were added, respectively. The plate was covered with Plate Sealer and incubated for 21 h at 37 °C at the low-shake function for a total of 24 measurements.

An additional 24-well plate of which only the two middle rows were used was filled with 1.5 ml of BHI broth and 7.5 μl of *S. aureus* pre-culture. One of the rows was used as a control while the other contained 5 kBq of Ra-223 in each well. The plate was covered with Plate Sealer and incubated for 18 h at 37 °C at the low-shake function for a total of 20 measurements.

2.5.5. Radium uptake

To measure the uptake of Ra-223 by *S. aureus*, the incubated well plate from the last step in Section 2.5.4 was used. The 6 well plates containing the irradiated *S. aureus* were pipetted into 1.5 ml screwcap microtubes. The initial activity in the samples was measured on the Wallac. The microtubes were then centrifuged at 4000 rpm and 5°C for 10 min. The supernatant was pipetted out and stored in a separate glass counting vial for each microtube. The resulting pellet was resuspended in 300 μl of 50 mM Tris-HCl solution with a pH of 8.0. The solution was again centrifuged at 4000 rpm and 5°C for 10 min. The supernatant was pipetted out and added to the same counting vial as in the previous step. The microtubes containing the resulting pellet and the counting vials containing the mixture of BHI broth and Tris-HCL were then measured in the Wallac to establish what part of the activity remained in the pellet.

The small volume of the pellet and the Wallac's sensitivity to sample geometry required to introduce a correction factor in the following way:

$$A_{corr} = \frac{A_{Wallac}}{1 - F_{corr}V_m} \quad (2.2)$$

Where A_{corr} is the corrected CPM, A_{Wallac} is the measured CPM, F_{corr} the correction factor in μl^{-1} and V_m the volume of the measured sample in μl . Therefore, an initial solution of 25 μl MilliQ and 2 μl Xofigo was measured on the Wallac. 100 μl of MilliQ was then added to the solution and the sample was measured again. This step was repeated 10 times in a final volume of 1027 μl .

The measured counts per minute for each volume were then plotted and a linear regression with the formula $A_{Wallac} = c_1 \cdot V_m + c_2$ was performed. F_{corr} is then defined as $F_{corr} = -c_1/c_2$ such that A_{corr} corresponds to the count rate measured with a filling volume of zero.

3

Results and Discussion

3.1. Release of radioactive isotopes from PMMA

The purpose of this series of experiments is to determine whether radioactive isotopes can be mixed into and subsequently released from low-viscosity PMMA.

3.1.1. Reproducible geometry

As part of the process of establishing the reproducibility of bone cement experiments, a variety of mixing containers and amounts of PMMA were used, as mentioned in Section 2.3.2. The mixing of PMMA in an agar plate did not yield a favorable result, as the resulting mixture could not be formed into a reproducible geometry. Smaller volumes of the mixture were mixed into a 6-well plate with the same result. Using a syringe to mix resulted in an uneven mixture, as the powder that first came into contact with the MMA would create a barrier for the liquid to penetrate further, and only a small amount of cement was formed, which also had a disproportionate ratio of liquid to powder. Mixing with the help of a needle through the tip of the syringe resulted in an even mix; however, when it came to depositing even amounts of mixed cement on a 48-well plate, the resulting cement fragments would have unequal volumes and surface areas. Furthermore, not all of the mixture could be deposited in time, as the cement hardens quickly enough that it becomes impossible to push it out of the syringe. Even if this method of creating a reproducible geometry of bone cement was successful, this method of handling would increase in difficulty once a radioactive isotope was added to the mixture. Therefore, it was deemed that this method is unusable for the aims of the project.

Ultimately, using a vortex to mix both components proved to be the most efficient. However, the larger Eppendorf tubes used produced inconsistent results because the mixture would spread too thin and unevenly along the conical bottom. The Safe Seal microtubes did result in a reproducible geometry with each mixture, with the added caveat that since they are much more narrow than the other two types, the liquid part of bone cement needed to be added first, so that all of the powder could come in contact with during mixing. This came with the added bonus that during later experiments, the radioactive MMA would be easier to handle, as when a vortex is used to mix it needs to be turned on almost immediately after the two parts come into contact to make a homogeneous mixture.

Five standard samples were mixed to measure the average dimensions. A sample of 27 mg of bone cement powder and 13.5 μl of MMA has a diameter of 4.07 ± 0.06 mm, volume of 27.64 ± 1.21 mm³ and a surface area (assumed to be a circle) of 3.29 ± 0.02 mm². The relevant dimensions for the sake of the experiments were an average diameter of 4.07 ± 0.06 mm, volume of 27.64 ± 1.21 mm³.

3.1.2. Powder to liquid ratio dependency

This particular experiment was carried out to determine if variations of the powder-to-liquid ratio have an effect on the amounts of Ga-68 release. The results of the activity obtained from the washes can be found in figure 3.1.

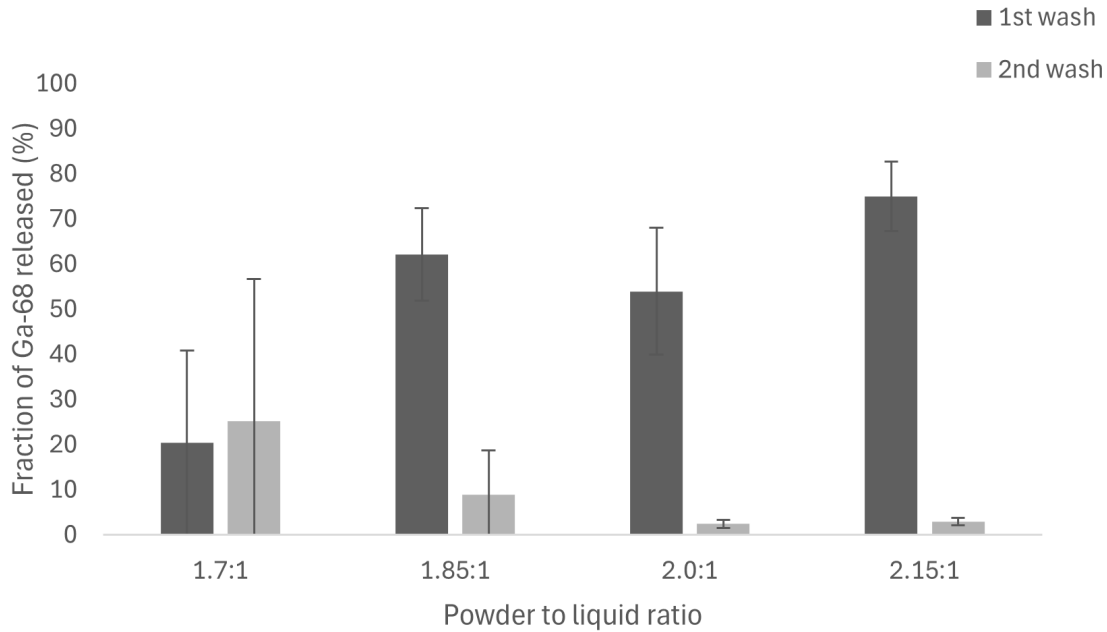


Figure 3.1: Release of gallium-68 from PMMA at four different powder:liquid mix ratios. The amount of liquid is kept the same while the amount of powder is varied. Error bars represent standard deviation of 3 separate experiments.

The activity in the figure is presented in % of the total amount loaded into the mixture, as the exact activity loaded into each sample can vary slightly. It can be observed that the mix ratio did not impact the total amount of gallium that was released during contact with the PBS. The mixtures of 1.85:1, 2:1 and 2.15:1 have comparable release with a large amount released at the first wash and only a small fraction on the 2nd. This could point to the gallium atoms not being bound inside the mix resulting in a massive release with the first wash. Another possible explanation is that during the vortexing of the mixtures, the Ga-HCl eluate might be rising to the surface and when PMMA starts to dry it settles there making it easy to wash away with liquid. However, the results for the 1.7:1 ratio point to something else. The large error present for this mix ratio is due to one of the samples releasing barely any of the gallium into the PBS which contradicts the loosely bound gallium hypothesis, because a lower amount of powder would suggest a softer, more porous bone cement and therefore more loosely bound gallium. Since no strong effect of the powder to liquid ratio was observed in this experiment, the ratio for all following PMMA experiments was kept 2:1.

3.1.3. Release dependency on contact time

To test whether contact time with PBS also influences the amount of Ga-68 released, an experiment similar to the previous one was conducted this time by varying contact time with PBS between 1 and 20 min. Data from the contact time experiment can be observed in figure 3.2. For all contact times, each consecutive wash results in a lower fraction of the gallium released from the PMMA. For contact times of 5, 10 and 20 min, the trend is that longer contact time results in a lower amount of released gallium for each wash. However, this is misleading as the data for 1 min of contact time does not follow this trend. Moreover, the large errors for contact times of 1 and 20 minutes are, similarly to results from Section 3.1.2, due to samples with little to no release of gallium. These results prompted further exploration of the interaction between PMMA and the gallium eluate.

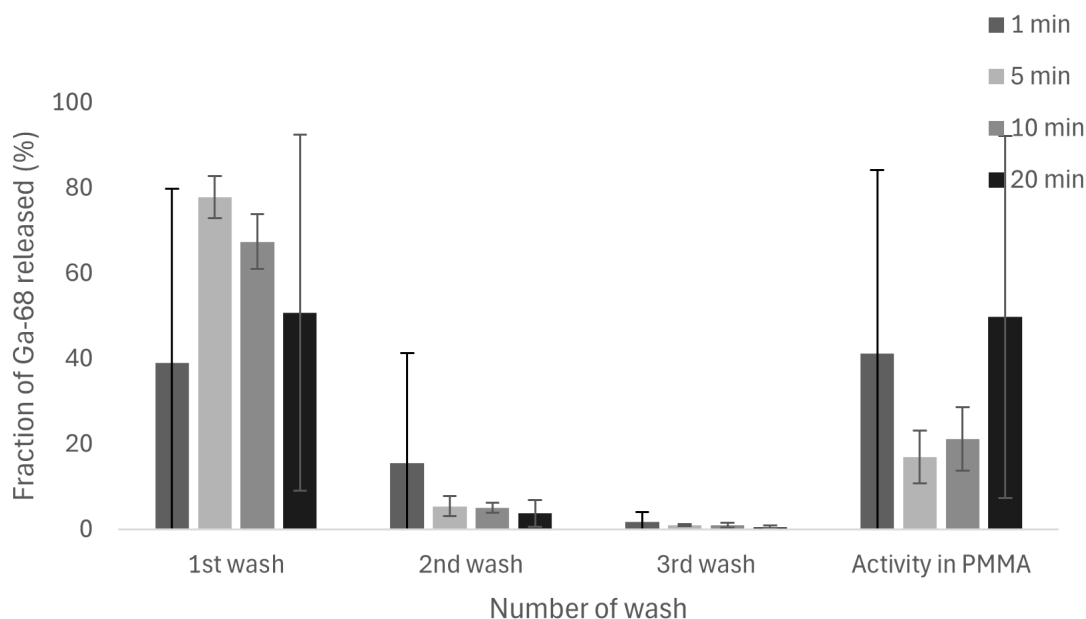


Figure 3.2: Release of gallium-68 from PMMA. The figure shows release of the radioisotope into PBS for 3 consecutive washes and four different contact times between PBS and PMMA. Error bars represent standard deviation of 3 separate experiments.

3.1.4. Solubility of Ga-68

The recurring zero-release samples from 3.1.2 and 3.1.3 pointed to the fact that in certain cases, the gallium mixed with the PMMA would be released in substantial amounts and in others barely at all. It was hypothesized that the Ga-HCl eluate was not soluble in MMA. This would mean that whether or not gallium release would occur depended largely on luck in previous experiments.

To test this hypothesis, the solubility of the Ga-68 eluate from the generator was tested in water and MMA, and subsequently the chelator N-benzoyl-N-phenylhydroxylamine (BPHA) was added to the MMA and the solubility was tested again. The results are summarized in table 3.1.

	MilliQ	MMA	BPHA-MMA
Fraction of activity (%)	10.16±0.54	0.12±0.04	13.46±0.67

Table 3.1: Percentage of total activity contained in a 10% fraction of solution volume for Ga-HCl in MilliQ, MMA and BPHA-MMA respectively.

The results of the mixing of Ga-HCl with MilliQ showed that the eluate is completely soluble in water with each sample taken from the solution producing 10% of the activity. The opposite was true when Ga-HCl was added to MMA, where the 100 μ l droplet of Ga-HCl eluate was visible with the naked eye sitting under the MMA in the Safe Seal microtube. Since the amount of Ga-68 used in the previous experiments was only 1 μ l, its insolubility became evident only when larger amounts were used. Samples of the Ga-HCl-MMA mixture were taken from the top layer and yielded almost no activity, as is seen in the table.

Repeating the same experiment, but adding BPHA as chelator to the MMA, led to equal amounts of Ga in each sample taken from the solution. This came out to around 13.5%. This initially did not make sense, since only 10% of the solution was pipetted out for each measurement. However, since 100 μ l of Ga-68 was added for this experiment, the measurement of total activity in the solution could have exceeded the accurate count limit of the Wallac. Since the deviation between measured samples was low, this is the most likely explanation for the discrepancy and the reason why the experiment was not

redone with a lower dose.

The results of these two experiments would explain the zero-release samples from the previous sections, as it would probably mean that the gallium got trapped inside the PMMA. However, samples that release a large amount of gallium into the PBS most likely had gallium near the contact layer between PMMA and PBS.

3.1.5. ^{68}Ga -BPHA contact time

With the addition of BPHA, the contact time experiment of Section 3.1.3 was repeated for contact times of 5 and 20 minutes. Figure 3.3 shows almost no release of Ga-68, which is exactly opposite to the massive release measured when no BPHA chelator was present in the mixture.

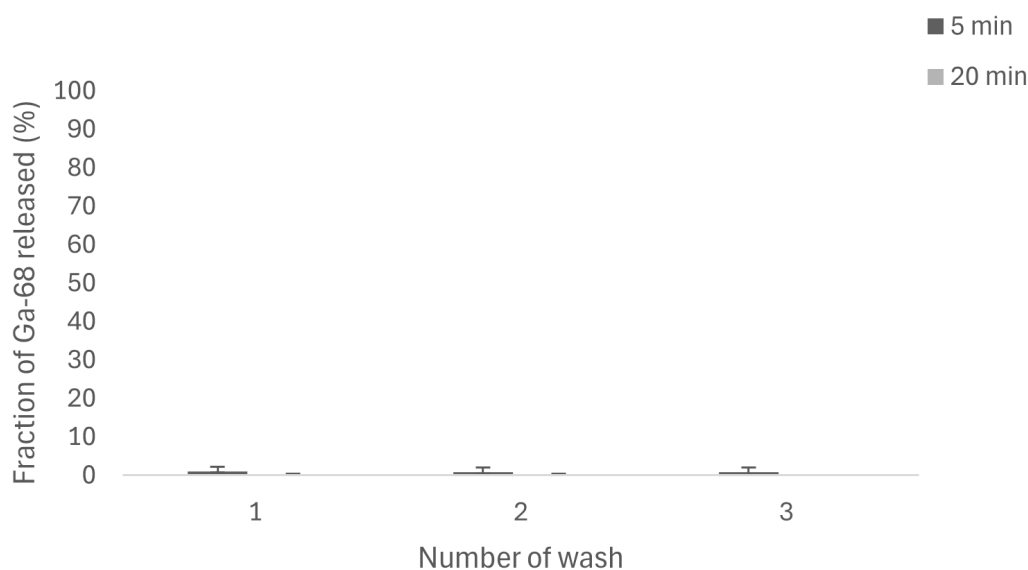


Figure 3.3: Release of gallium-68 from PMMA with the presence of BPHA. The figure shows release of the radioisotope into PBS for 3 consecutive washes for two different contact times between PBS and PMMA. Error bars represent standard deviation of 3 separate experiments.

Almost no gallium is released from solid PMMA with slightly more release in the case of 5 minutes of contact time (a total of 3%). Assuming that the inclusion of BPHA results in the isotope being homogeneously distributed throughout the PMMA volume, it could be that the activity needs to be much higher for there to be a measurable amount of release. Higher activity could be achieved by increasing the concentration of BPHA, however, the amount of 42.6 mg used for this experiment is already 2.1% of the total powder mass, which is close to the 2.3% concentration of gentamicin found in the antibiotic loaded version of the same bone cement [58]. As mentioned in Section 1.2 higher concentrations of antibiotics and, in general, other substances in the cement mixture contribute to unfavorable mechanical properties [14],[16]. Another constraint of gallium in this case is its relatively short half-life, making any long-term contact times impossible.

In comparison, the release of gentamicin for the same bone cement brand reported in the literature seems to be mixed. Similarly to the methodology described in Section 2.3.2., a study carried out with Palacos R bone cement immersed in PBS reported an initial spike in gentamicin release in the first few hours followed by a rapid decrease [59]. The total amount of gentamicin released in 70 h was $70 \pm 3.2 \mu\text{g}$ which was only 8.4% of the total amount contained in the cement. This trend of high initial release is similar to the results reported for the release of Ga-68 without the inclusion of a chelator. However, the total amount released is much lower, as the minimal amount of Ga-68 released was 50% (Fig. 3.2). Another study comparing the release of gentamicin in PBS from multiple brands of PMMA, including

Palacos R + G, found that antibiotic concentrations in PBS had a relatively low initial value ($1 \mu\text{g}/\text{ml}$ for Palacos R + G), which increased slowly over the course of 150 h to around $20 \mu\text{g}/\text{ml}$ [60]. This is in contrast to the aforementioned study, as a slowly rising concentration would mean a sustained release throughout the experiment. It is possible that Ga-68 with the inclusion of BPHA would release similarly, however, its short half-life would make such an experiment impossible.

3.1.6. Ra-223 release from PMMA

The next step in the investigation of PMMA as a possible carrier of radioisotopes was to load Ra-223 into the cement and measure its release over time. The results of the two experiments performed simultaneously are shown in Fig. 3.4 below.

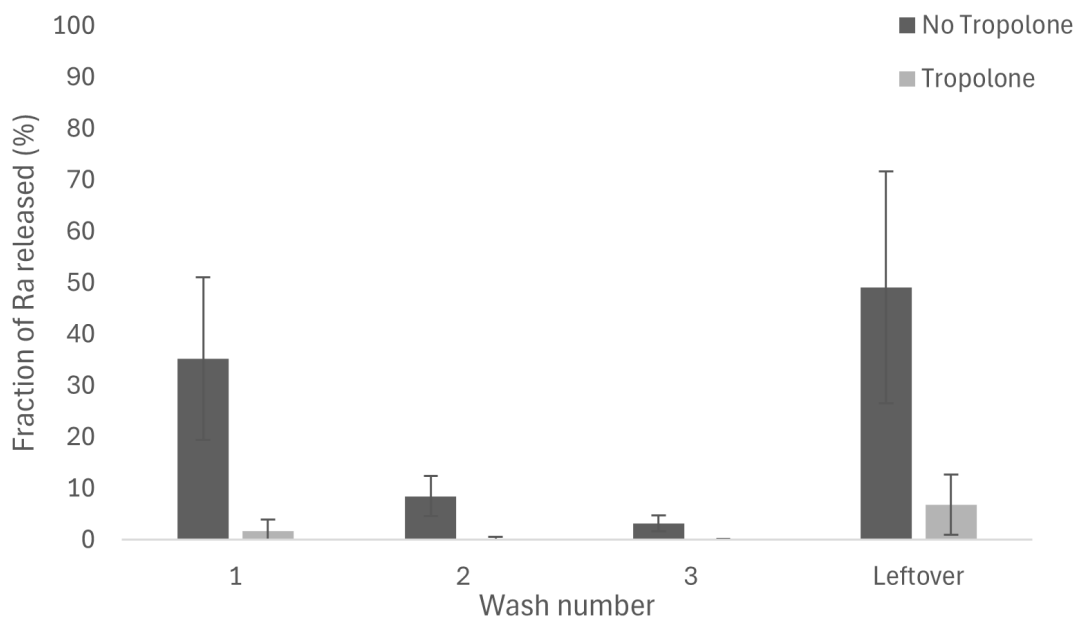


Figure 3.4: Release of Ra-223 from PMMA with and without the presence of tropolone. The figure shows release of the radioisotope into PBS for 3 consecutive washes and a contact time of 1 day. Error bars represent standard deviation of 3 separate experiments.

The non-tropolone batch shows a significant initial release of Ra-223 in the first wash and a smaller, but noticeable release in the second and third. Overall, this result aligns with the result for Ga-68 when no chelator was present. This was expected as Xofigo is a water-based solution and therefore does not mix with the MMA liquid. The dispersal and position of the activity within the cement are non-homogeneous and likely determined by the vortexing of each sample.

The more interesting result is for the batch containing the chelator tropolone. Although the release measure for the three washes is similar for those of Ga-68 when BPHA was added as chelator, the residual activity measured in the PMMA after the third wash was only $6.83 \pm 5.82\%$ of the initial activity. This result, combined with the total amount of release measured, added up to under 10% of the initial activity even when corrected for decay. This was in contrast to every other PMMA isotope release experiment where the sum of the leftover and wash activities matched the initial measurement. The relatively large error bars for the first wash and residual activity for the tropolone batch were in fact due to only one of the samples containing a tiny amount of Ra-223, the other two being effectively zero. This meant that what was being measured as the initial activity of Ra-223 was not actually due to the presence of Ra-223, but to another isotope. This result was confusing, as the Wallac measures using a specific protocol for each isotope designed with a custom energy range, and so measuring with the protocol for Ra-223 and Rn-219 no other isotope peaks from the Ra-223 decay chain should have been measured.

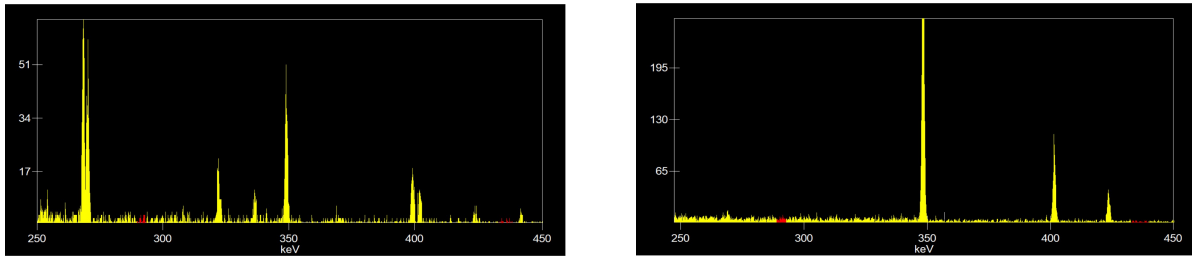


Figure 3.5: Gamma spectrum of two PMMA samples. The left figure corresponds to a sample in which pure Xofigo was added, while the right figure corresponds to the spectrum of PMMA for which tropolone was used to extract Ra-223 from Xofigo. The y-axis represents total counts.

These results prompted to measure one sample of the non-tropolone batch and a fresh sample with tropolone on a germanium detector. The germanium detector has a higher resolution than the Wallac and would help separate each gamma peak of the entire Ra-223 decay chain. The results for both samples can be observed in Fig. 3.5 below.

For a more clear view, the energy range was limited to energies ranging from 250 to 450 keV, as this is where the majority of the gamma peaks of the Ra-223 decay chain are found. The figure on the left shows a multitude of peaks, of which the two peaks between 250 and 300 keV, the peak just below 350 keV, and the peak right after 400 keV are most important. These peak correspond to Ra-223 at 269 keV, Rn-219 at 271 keV, Bi-211 at 351 keV, and Pb-211 at 404 keV [61].

As can be seen in the figure on the right, many of the peaks are missing, but most notably the two peaks at 269 and 271 keV. This means that no Ra-223 or Rn-219 were present in the tropolone sample. The remaining three peaks point to the presence of Pb-211 and Bi-211. Since Bi-211 is a daughter nuclide of Pb-211, the most likely explanation as to why the Wallac measured activity in the tropolone samples even without Ra-223 present is that only Pb-211 was extracted by the tropolone when vortexing MMA and Xofigo. This led to the Wallac, due to its poorer resolution, measuring part of the Bi-211 peak while using a protocol for Ra-223 and Rn-219 and some activity being measured with the protocol for Pb-211. This would also explain why measurements following the initial one resulted in 0 activity since Pb-211 has a half-life of only 36.1 min. This result is not surprising, as the choice of tropolone as the chelator was driven by its organic solubility and not its chelating properties. tropolone is typically used to chelate 3+ ions while radium is a 2+ ion; however, the only suitable chelator available was Macropa which is an aqueous soluble chelator and would not have mixed with the organic MMA [62].

3.2. Growth of *S. aureus* in the presence of Ra-223

3.2.1. Establishing a baseline and choosing a suitable well plate cover

With this initial series of experiments, the objective was to obtain data on how *S. aureus* grows without the presence of Ra-223 with different materials covering the well plate while inside the PowerWave XS plate reader. This was done to determine which well plate cover would best reduce growth medium evaporation and also limit contamination with Ra-223.

Initially, six wells on a 24-well plate were cultured and data points were obtained from the PowerWave XS plate reader. This data served to construct a baseline growth curve. After this, a new 24-well plate was used to test the two covers. The results for the three data sets are shown in Fig. 3.6 where the growth curves were constructed using the Slogistic1 model in OriginPro®.

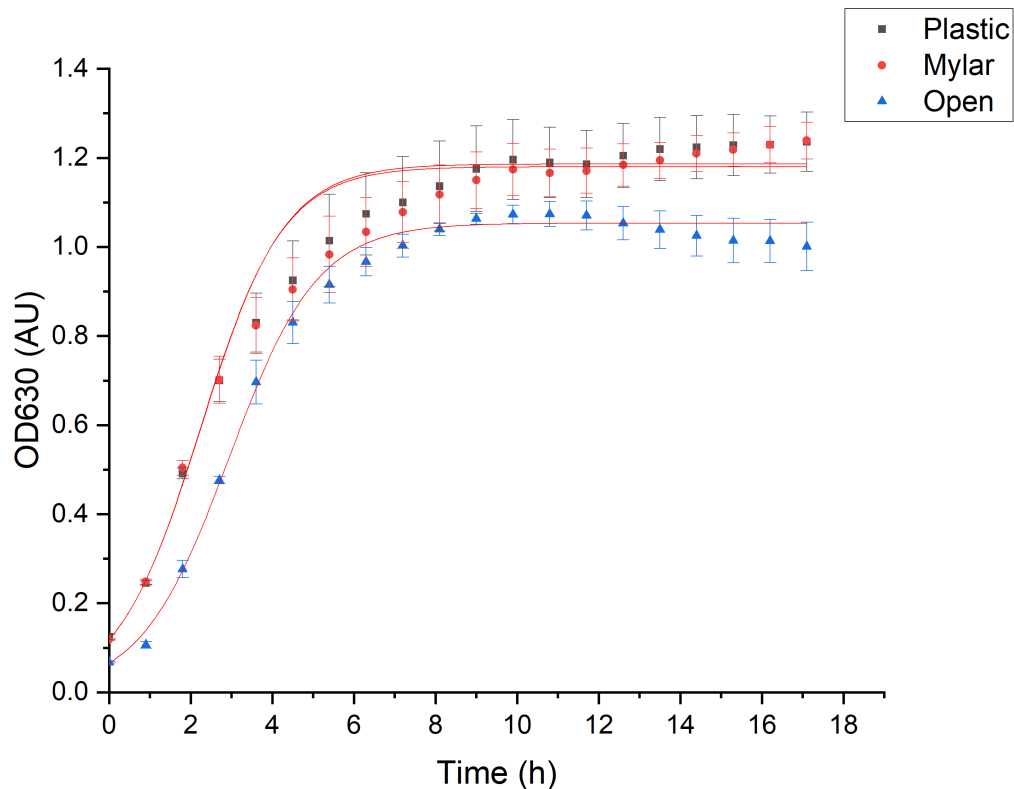


Figure 3.6: Growth curves of *S. aureus* obtained through OD630 measurements during incubation at 37°C and low-shake for 18 h in a well-plate reader. Each dataset corresponds to a different material covering the wells. Data points are an average obtained from six individual wells. Error bars represent their standard deviation.

Growth of *S. aureus* under mylar and a plastic well plate cover appears to be nearly identical with overlap between data points and growth curves. The estimated growth parameters in Table 3.2 suggest a similar conclusion. Compared to the baseline growth curve, the data suggest that the bacteria reach a higher population density when in a closed environment; however, there is a slight but meaningful difference in the initial bacterial concentration measured.

An interesting detail to note is how data points for the open well plate show a decrease in the OD630 value after around the 9 h mark. This could be due to partial evaporation of the BHI medium and, therefore, to a shorter light path. Since optical density measurements are performed based on the Beer-Lambert law, a difference in the light path between the measurements would lead to different values of optical density [63].

Instructions posted on the website of the plate reader manufacturer BML LABTECH on how to optimize

OD600 measurements point to several factors that could lead to a change in optical density. According to the instructions, evaporation of the growth medium due to an uncovered well plate can lead to the osmolarity of the medium surrounding the microbes changing beyond the optimal level and leading to a reduced growth rate. Their data show that over 40% of the liquid medium evaporates over the course of 12 h of incubation at 37° C, while the liquid volume of the sealed well plate remains close to 100% [64]. In contrast, a study by Chavez et al. on the effects of different well plate covers found that while covering the well plate with a lid or a plate sealer can lead to different evaporation rates, this had no observable effect on the growth dynamics of bacteria [65]. However, the type of cover led to different OD600 measurements, with cultures covered with a lid reaching higher OD600 values overall, possibly due to the higher evaporation measured with this type of cover [65]. According to BMG LABTECH, condensation formed on the lid or sealer of a microplate can artificially increase optical density readings by scattering light [64].

Given this information, there are a few possible explanations for the observed results in Fig. 3.6. The initial bump in OD630 for the covered wells could be explained by the additional scattering by the cover. This would mean that every data point would have a slightly larger value than the corresponding open well data point. Another explanation for the discrepancy in the initial value is a difference in bacteria concentration; however, this is less likely because every culture was prepared using a fresh preculture incubated under the same conditions. Furthermore, when the measurements were concluded, it was discovered that condensation had formed over each well containing a bacterial culture. This condensation would lead to higher OD630 measurements, which could explain the difference in the growth pattern after the 9 h mark between closed and open well plates depending on when condensation started to form on the plate sealer and Mylar sheet. It is possible that open well plate evaporation led to lower bacteria growth, but the literature appears inconclusive on whether evaporation negatively affects growth or does not affect it at all.

Type of cover	OD _{630,max} (AU)	μ_{max} (h ⁻¹)	t _i (h)
Open	1.05±0.01	0.92±0.02	2.94±0.05
Plastic	1.19±0.02	0.98±0.04	2.25±0.06
Mylar	1.18±0.02	0.98±0.03	2.23±0.07

Table 3.2: Estimated growth parameters of *S. aureus* cultured without radium in an open well plate (No cover) and two types of covers (Plastic and Mylar).

Given that results for both covers were similar, the choice of cover for the following experiments was a matter of convenience, and therefore, the plastic well plate cover was chosen.

An intermediate test was conducted to determine whether there was any activity leaking into neighboring wells in the presence of a well plate cover. The diagram in the following (Fig. 3.7) shows the setup in which a single well with activity was surrounded by wells filled with MilliQ. After the well plate was run through the well plate reader, the liquid of each well was measured, and no amount of activity was present in the surrounding wells. This means that the well plate cover sufficiently isolates neighboring wells, and it will be assumed that changes in activity for each well plate are only due to decay of the isotope.

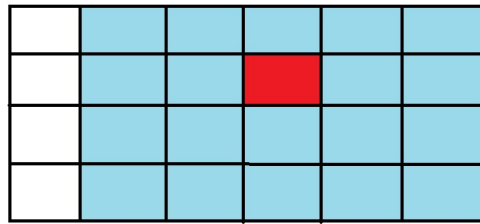


Figure 3.7: Schematic of the cross-contamination test setup. The red square represents the well containing activity while blue represents the surrounding wells filled with water.

3.2.2. Growth curve experiments

With the choice of a plastic cover for the well plate, bacteria were once again grown in the well plate reader, this time for 21 h and with different amounts of Ra-223 activity added, results of which are in Fig. 3.8.

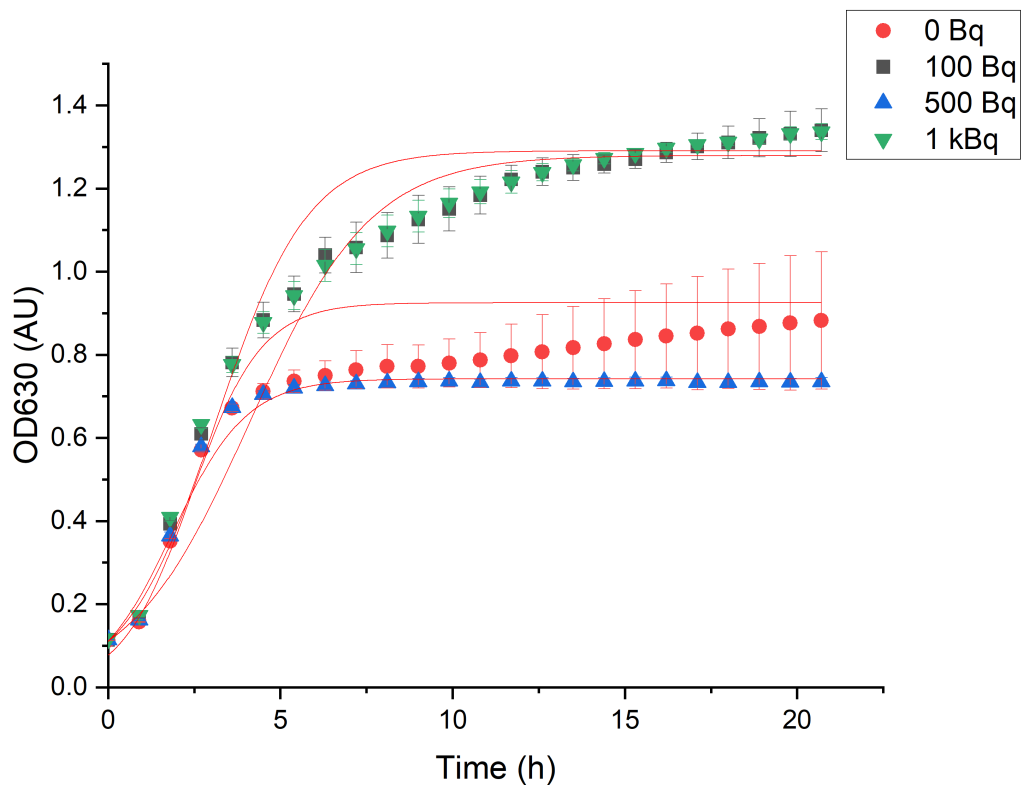


Figure 3.8: Growth curves of *S. aureus* under different activities of radium-223 and the well plate covered with a Plate Sealer, obtained by OD630 measurements and incubation time of 21 h. The four growth curves are obtained from a single well-plate with each row of wells containing a separate activity. Error bars represent standard deviation of 4 separate experiments for the 100 Bq dataset and 5 for the rest.

As can be seen in Fig. 3.8, there are two distinct groups. The 100 Bq and 1 kBq with the highest growth and the 500 Bq and control samples with the lower OD630 values. This was likely due to the 100 and 1 kBq groups being in the border rows of the well plate where the cover had been peeled off and the medium evaporated slightly. Therefore, only samples within each group had comparable parameters as shown in Table 3.3. It is important to mention that while the growth curves on Fig. 3.8 appear to not fit the data points entirely, the R^2 values, 0.94, 0.97, 0.99 and 0.99 for 0, 100, 500 and 1000 Bq

respectively, reflect a good overall fit of the Slogistic1 model.

Initially, the full set of data resulted in large, overlapping error bars between samples with different activities. This was due to the plate cover being slightly peeled on one of the short sides of the well plate, leading to evaporation in 4 of the wells. For the 100 Bq samples, there was a single outlier that did not show any growth until the 6 h mark, after which it experienced rapid growth and caught up with the rest of the wells for that activity. This could be due to a fault in the plate reader as the same OD630 was measured for the first 7 reads. Due to these outliers and the fact that each row contains 6 samples, the 4 side wells as well as the single outlier in the 100 Bq samples were excluded to have a more accurate idea of what was going on with the rest of the wells. The graph resulting from the full dataset can be found in Appendix A.

The lower OD630 group shows that the 500 Bq sample had a lower growth than the control, which could point to a possible effect of radium-223 on *S. aureus*, however the large errors for the control make that uncertain. In the case of the higher OD630 group, the higher growth curve belongs to the 1 kBq samples, which is contraindicative to the lower OD630 group. This is also reflected in the μ_{max} values in Table 3.3 where bacteria growing with 500 Bq of Ra-223 had a lower maximum growth rate than the 0 Bq group, while the opposite is true for the 100 Bq and 1 kBq groups.

An important note here is that for all four activities, the initial OD630 is relatively close to the initial value of the covered well plate in Fig. 3.7 of around 0.1. This means that the bump in the initial value could really be attributed to the presence of a cover.

Amount of ²²³ Ra activity	OD _{630,max} (AU)	μ_{max} (h ⁻¹)	t _i (h)
0 Bq	0.93±0.11	0.99±0.09	2.41±0.28
100 Bq	1.28±0.05	0.57±0.04	4.12±0.29
500 Bq	0.74±0.01	0.93±0.06	1.87±0.12
1 kBq	1.29±0.02	0.75±0.04	3.15±0.15

Table 3.3: Estimated growth parameters of *S. aureus* cultured in the presence of different activities of radium-223 with the well-plate covered with a plastic cover.

To determine whether activity actually impacts growth, another well plate was cultured this time using 7.6 kBq. Only the two middle rows of the well plate were cultured to avoid the previously observed peeling of the edges of the cover.

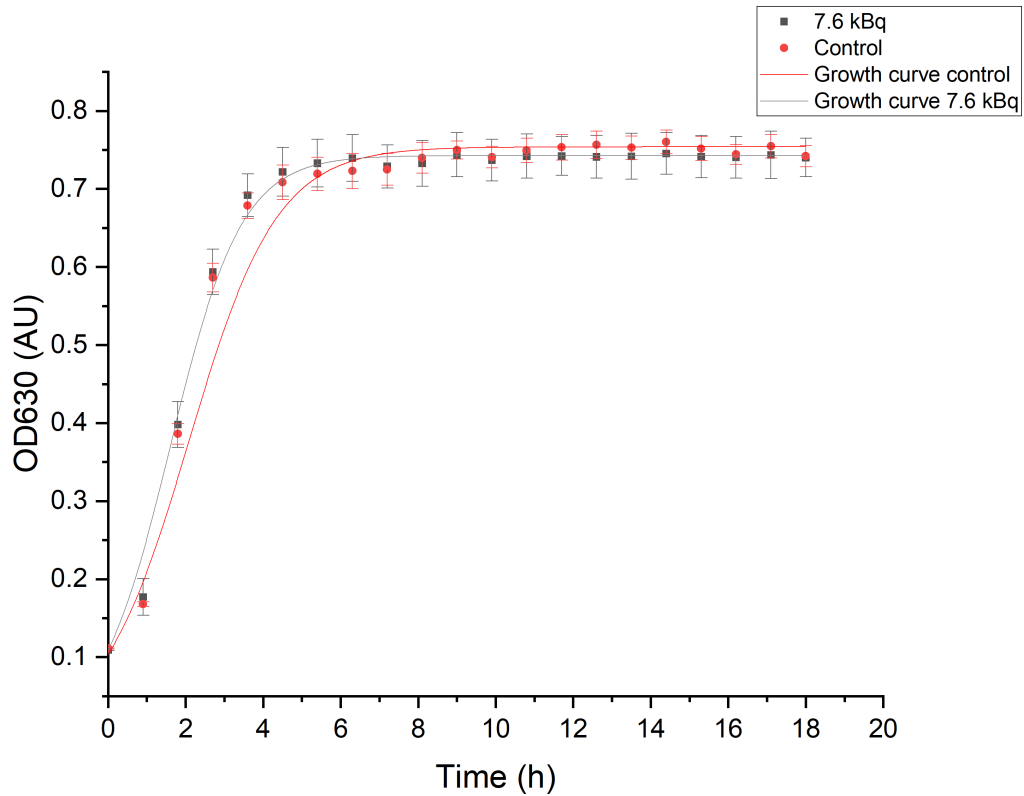


Figure 3.9: Growth curves of *S. aureus* in presence of radium-223 and the well plate covered with a Plate Sealer, obtained by OD630 measurements and incubation time of 18 h. The two growth curves are obtained from a single well-plate with each row of wells containing a separate activity. Error bars represent standard deviation of 5 separate experiments.

As shown in Fig. 3.9, both the control and 7.6 kBq samples have similar growth curves, as also reflected in the growth parameters in Table 3.4. These parameters can be compared with the parameters in the first and third rows of Table 3.3, which in theory have the same growth conditions. The main differences in the two growth curves is that the maximum growth rate is higher for the samples containing radium, but also its inflection time is shorter, meaning its growth starts decreasing earlier than the control.

This is not the case when comparing them with the growth parameters in the first and third rows of Table 3.3 where the samples containing activity have a lower maximum growth rate and a shorter inflection time at the same time. However, these differences may be attributed to the larger errors in Fig. 3.8, as opposed to Fig. 3.9, where both the control and the 7.6 kBq samples overlap in data points and error bars.

Sample	OD _{630,max} (AU)	μ_{max} (h ⁻¹)	t _i (h)
Control	0.75±0.01	0.88±0.06	2.09±0.14
7.6 kBq	0.74±0.01	1.09±0.03	1.61±0.05

Table 3.4: Estimated growth parameters of *S. aureus* cultured with two different activities present.

The apparent lack of bactericidal effect against *S. aureus* even in the case of 7.6 kBq may be due to the fact that the dose is still far too low to have any significant effect. With the total volume of each culture being 1517.5 μl , this means that the activity concentration in each sample is 5 Bq per μl . For comparison, in the study mentioned in Section 1.7 that showed that Bi-213 had a significant bactericidal effect on planktonic bacteria, 370 kBq of activity was used [51]. This is much more than would have

been permissible for the sake of the experiments outlined in this thesis and could explain the lack of bactericidal effect in this case.

3.2.3. Uptake of Ra-223 by *S. aureus*

A further cause of the lack of effect could be that the uptake of radium is not high enough to kill a significant number of bacteria to curb colony growth. Therefore, another set of colonies was grown for 18 h with 5 kBq per well added and bacterial cells were separated from the culture medium to measure the activity contained inside.

After two rounds of centrifugation, only $8 \pm 5\%$ of the total activity added to the samples was taken up by the bacteria. After determining the correction factor for the sample volume as $F_{corr} = 0.00014 \pm 0.00001 \mu\text{l}^{-1}$ and applying it to the count rates of the pellet and liquid fractions the resulting measured uptake decreased to $6 \pm 4\%$. This means that of the 5 kBq, only about 300 Bq ended up inside bacterial cells where they have the chance to kill them. The low uptake would explain the lack of a measurable bactericidal effect observed in all previous growth experiments. As a rough estimate, the average diameter of an *S. aureus* cell is $1 \mu\text{m}$ making the average volume $0.52 \mu\text{m}^3$ [66]. A study by Mira et al. calibrated OD600 measurements to the concentration of cells for different bacterial species and found that an OD600 of 1 for *S. epidermidis* (with an average volume of $1 \mu\text{l}^3$ was equal to a concentration of $3.42 * 10^{10}$ cells/ml [67]. In general, none of the bacteria mentioned in this study had a concentration lower than 10^8 cells/ml and they were all larger in volume than *S. aureus*. This points to the concentration of cells in this experiment being also in the order millions of cells/ml making the amount of 300 Bq absorbed Ra-223 insignificant.

4

Conclusions and recommendations

4.1. Conclusions

The objectives of this thesis were to establish whether or not PMMA can be used as a delivery vehicle for radioactive isotopes such as Ga-68 and Ra-223, to test the bactericidal effect of Ra-223 on *S. aureus* as well as to measure the uptake of Ra-223 by *S. aureus*.

To achieve the first objective, a mixing procedure resulting in reproducible geometry was established for all experiments involving PMMA. Different powder-to-liquid ratios were investigated to determine the effect of mixing ratios on Ga-68 release. The contact time of the loaded PMMA with PBS was also investigated to measure if increased contact time would result in more of the Ga-68 being released. The results of both experiments were inconclusive as anomalous samples skewed the measured release. This prompted an investigation into the solubility of the Ga-68 eluate with MMA. Measurements of 10% fractions from the volume of a ^{68}Ga -MMA mixture showed that each fraction contained $0.12 \pm 0.04\%$ of the total added activity, whereas when mixed with water $10.16 \pm 0.54\%$ of the total activity was measured. This meant that the eluate was soluble in water but not in MMA. The addition of BPHA, an organic soluble chelator, solved this problem; however, this negatively affected the release of Ga-68, as the total release for a contact time of 5 min decreased from 83% to 3%. Conducting similar experiments for Ra-223 with and without a chelator, which was tropolone in this case, resulted in similar release. Greater release was observed when no chelator was present, but the addition of tropolone resulted in almost no release, as the chelator had bound to the daughter nuclide Pb-211 instead of Ra-223.

The second objective of measuring the bactericidal capacity of Ra-223 was carried out by first choosing an appropriate cover for the well plate to minimize evaporation and contamination with Ra-223. To test the effects of Ra-223 on *S. aureus* cultures, three different activities of 100, 500 and 1000 Bq were used. Since the plastic plate sealer had partially separated from the well plate, the data sets were treated as two groups, one being 0 Bq and 500 Bq, which had not evaporated, and the other 100 Bq and 1000 Bq, which had partially evaporated. The growth curves for the non-evaporated group showed slightly lower growth when activity was present, $OD_{630_{max}}$ being $0.93 \pm 0.11 AU$ for bacteria growing without Ra-223 and $0.74 \pm 0.01 AU$ for bacteria with Ra-223. For the partially evaporated group, a difference was found only in inflection time and maximum growth rate, where $t_i = 4.12 \pm 0.29$ h and $\mu_{max} = 0.57 \pm 0.04$ h^{-1} were the parameters of the 100 Bq batch and $t_i = 3.15 \pm 0.15$ h and $\mu_{max} = 0.75 \pm 0.04$ h^{-1} for the 1 kBq batch. The same experiment was repeated with a higher activity of 7.6 kBq, which resulted in the following differences in growth parameters between the two groups: $t_i = 2.09 \pm 0.14$ h and $\mu_{max} = 0.88 \pm 0.06$ h^{-1} for the control group and $t_i = 1.61 \pm 0.05$ h and $\mu_{max} = 1.09 \pm 0.03$ h^{-1} for the 7.6 kBq group. The uptake of Ra-223 was measured with an activity of 5 kBq of Ra-223. Two consecutive centrifugations were performed to separate the bacterial mass from the growth medium. The activity contained in the bacterial pellet was estimated at $6 \pm 4\%$, which is approximately 300 Bq. This result explained the lack of effect on bacterial growth as the initial concentration of bacteria is likely in the millions of cells/ml.

In conclusion, PMMA has the potential to carry radioactive isotopes; however, the solubility of the

isotopes in MMA and the potential use of the appropriate chelator could have a great impact on the release profile. The results on the bactericidal ability of Ra-223 against *S. aureus* were inconclusive. Further experiments would benefit from increasing the activity of Ra-223 used to ensure that there is a sufficient amount taken up by the bacteria to draw any conclusions about its bactericidal effect.

4.2. Recommendations

In this chapter, several recommendations are made to further test the viability of PMMA as a delivery vehicle for Ra-223, as well as the bactericidal capacity of Ra-223 against *S. aureus*. Some suggestions for experiments are also given to elaborate on the findings reported in this thesis.

First, an appropriate organic-soluble chelator should be used to extract Ra-223 from its aqueous solution and transfer it to methyl methacrylate to obtain similar results to those for the release of Ga-68 when BPHA was present as the chelator. Because the isotope would be homogeneously distributed throughout the PMMA, it would be interesting to see whether the powder-to-liquid ratio would have an effect on the release in this case. As all PMMA experiments in this thesis were performed at room temperature (21 °C), while most experiments in the existing literature are performed at a temperature of 37°C, the effect of temperature on Ra-223 release should also be investigated. This would make results more easily comparable with others in literature. Furthermore, the mechanical properties of PMMA mixed with a radioisotope should also be studied as the inclusion of such materials could affect the overall viability of PMMA as a delivery vehicle[14, 16].

When it comes to the bactericidal properties of Ra-223, it is possible that the plate reader was not the optimal method to measure growth in the presence of Ra-223. Therefore, it would be interesting to investigate whether the use of standardized cuvettes to measure optical density would produce similar results. The use of cuvetts would remove many of the variables such as accounting for the plate cover impacting optical density measurements as well as evaporation and condensation impacting the growth and measurements. Furthermore, there are other methods for measuring growth, such as colony counting, that may prove useful as a comparison to the OD630 method used in this thesis. In general, incubation times can be reduced to 10 hours to more closely monitor the exponential phase of the growth, as this would produce similar results and save a significant amount of time.

Furthermore, using Ra-223 activities much higher than those used in this thesis could make its effect (or lack thereof) on *S. aureus* much more evident. Investigations of internalization of Ra-223 and its daughters by *S. aureus* could also be important as this could help optimize and increase uptake.

Outside of the scope of this thesis, the effect of Ra-223 on *S. aureus* biofilm should be studied, as the bacteria in the biofilm behave in a completely different way than planktonic bacteria. Experiments combining biofilm and Ra-223 loaded PMMA could potentially have very different results than those observed in this thesis, as bacteria inside the biofilm have multiple defenses against antibacterial agents ranging from a mechanical barrier to increased adaptability. Furthermore, since bacteria and biofilm are expected to be encountered on or near the surface of bone cement, efforts should be focused on limiting the inclusion of Ra-223 near the surface of PMMA, as this is the main area where an alpha emitter would have the greatest chance of encountering and internalizing by the bacteria. Numerous antibacterial coatings for implants are being actively investigated and the incorporation of Ra-223 into these coatings could be a viable option for a more controlled release of the alpha emitter on the surface of implants [23, 34]. Another way in which not only Ra-223, but other alpha emitters as well could be used to treat infections is by attaching them to antibodies for a highly targeted approach [52]. As a final remark, the treatment of infections is rarely approached using a single modality. Research of alpha emitters as possible antibacterial agents should be done in conjunction with other methods, since a modality on its own is rarely as effective as a multipronged approach.

References

- [1] Anubhav Bussooa, Steven Neale, and John R. Mercer. "Future of Smart Cardiovascular Implants". In: *Sensors* 18 (July 2018), p. 2008. DOI: 10.3390/s18072008. URL: <https://www.mdpi.com/1424-8220/18/7/2008/htm>.
- [2] Wahid Khan et al. "Implantable Medical Devices". In: *Advances in Delivery Science and Technology* (Dec. 2013), pp. 33–59. DOI: 10.1007/978-1-4614-9434-8_2. URL: https://link.springer.com/chapter/10.1007/978-1-4614-9434-8_2.
- [3] A Kashi and S Saha. "Failure mechanisms of medical implants and their effects on outcomes". In: *Elsevier eBooks* (Jan. 2020), pp. 407–432. DOI: 10.1016/b978-0-08-102680-9.00015-9. (Visited on 08/02/2024).
- [4] Luis Pulido et al. "Periprosthetic Joint Infection: The Incidence, Timing, and Predisposing Factors". In: *Clinical Orthopaedics and Related Research* 466 (Apr. 2008), pp. 1710–1715. DOI: 10.1007/s11999-008-0209-4.
- [5] Carla Renata Arciola et al. "Biofilm formation in Staphylococcus implant infections. A review of molecular mechanisms and implications for biofilm-resistant materials". In: *Biomaterials* 33 (Sept. 2012), pp. 5967–5982. DOI: 10.1016/j.biomaterials.2012.05.031. (Visited on 07/19/2019).
- [6] Steven M. Kurtz et al. "Economic Burden of Periprosthetic Joint Infection in the United States". In: *The Journal of Arthroplasty* 27 (Sept. 2012), 61–65.e1. DOI: 10.1016/j.arth.2012.02.022.
- [7] Lucio Montanaro et al. "Scenery of Staphylococcus implant infections in orthopedics". In: *Future Microbiology* 6 (Nov. 2011), pp. 1329–1349. DOI: 10.2217/fmb.11.117. URL: <https://pubmed.ncbi.nlm.nih.gov/22082292/> (visited on 11/24/2020).
- [8] Kaisa Huotari, Mikko Peltola, and Esa Jämsen. "The incidence of late prosthetic joint infections". In: *Acta Orthopaedica* 86 (Mar. 2015), pp. 321–325. DOI: 10.3109/17453674.2015.1035173. (Visited on 10/15/2020).
- [9] Ajay Premkumar et al. "Projected Economic Burden of Periprosthetic Joint Infection of the Hip and Knee in the United States". In: *The Journal of Arthroplasty* 36 (May 2021), 1484–1489.e3. DOI: 10.1016/j.arth.2020.12.005.
- [10] Honglue Tan et al. "Physical characterization and osteogenic activity of the quaternized chitosan-loaded PMMA bone cement". In: *Acta Biomaterialia* 8 (July 2012), pp. 2166–2174. DOI: 10.1016/j.actbio.2012.03.013. (Visited on 10/23/2019).
- [11] David J Apple. *Sir Harold Ridley and his fight for sight : he changed the world so that we may better see it*. Slack, 2006.
- [12] Umar Ali, Khairil Juhanni Bt. Abd Karim, and Nor Aziah Buang. "A Review of the Properties and Applications of Poly (Methyl Methacrylate) (PMMA)". In: *Polymer Reviews* 55 (June 2015), pp. 678–705. DOI: 10.1080/15583724.2015.1031377.
- [13] Todd Jaeblon. "Polymethylmethacrylate: Properties and Contemporary Uses in Orthopaedics". In: *American Academy of Orthopaedic Surgeon* 18 (May 2010), pp. 297–305. DOI: 10.5435/00124635-201005000-00006.
- [14] Khaled J. Saleh et al. "Acrylic bone cement in total joint arthroplasty: A review". In: *Journal of Orthopaedic Research* 34 (Feb. 2016), pp. 737–744. DOI: 10.1002/jor.23184.
- [15] A.J. Donaldson et al. "Bone cement implantation syndrome". In: *British Journal of Anaesthesia* 102 (Jan. 2009), pp. 12–22. DOI: 10.1093/bja/aen328.
- [16] Alessandro Bistolfi et al. "Antibiotic-Loaded Cement in Orthopedic Surgery: A Review". In: *ISRN Orthopedics* 2011 (Aug. 2011), pp. 1–8. DOI: 10.5402/2011/290851. URL: <https://downloads.hindawi.com/archive/2011/290851.pdf>.

- [17] Honglue Tan et al. "The use of quaternised chitosan-loaded PMMA to inhibit biofilm formation and downregulate the virulence-associated gene expression of antibiotic-resistant staphylococcus". In: *Biomaterials* 33 (Jan. 2012), pp. 365–377. DOI: 10.1016/j.biomaterials.2011.09.084. (Visited on 04/08/2021).
- [18] Elnaz Olyaei, Mohammad Mohammadzadeh, and Parisa Azimi. "Comparative study of Lutetium-177 and Phosphorus-32 in radioactive bone cement for the treatment of vertebral body metastasis". In: *Journal of Cancer Research and Clinical Oncology* 149 (Mar. 2023), pp. 7479–7491. DOI: 10.1007/s00432-023-04695-1. (Visited on 11/06/2024).
- [19] Carlos Julio Montaña and Maria Mendonça. "RADIOACTIVE CEMENT OF PMMA AND HAP-Sm-153, Ho-166, OR RE-188 FOR BONE METASTASIS TREATMENT". In: *Acta Ortopedica Brasileira* 27 (Feb. 2019), pp. 64–68. DOI: 10.1590/1413-785220192701190288. (Visited on 10/27/2023).
- [20] A VANBELKUM et al. "Co-evolutionary aspects of human colonisation and infection by *Staphylococcus aureus*". In: *Infection, Genetics and Evolution* 9 (Jan. 2009), pp. 32–47. DOI: 10.1016/j.meegid.2008.09.012.
- [21] Ruud H. Deurenberg and Ellen E. Stobberingh. "The evolution of *Staphylococcus aureus*". In: *Infection, Genetics and Evolution* 8 (Dec. 2008), pp. 747–763. DOI: 10.1016/j.meegid.2008.07.007. URL: <https://www.sciencedirect.com/science/article/pii/S156713480800141X>.
- [22] Donghui Zhang et al. "Dealing with the Foreign Body Response to Implanted Biomaterials: Strategies and Applications of New Materials". In: *Advanced Functional Materials* 31 (Oct. 2020), p. 2007226. DOI: 10.1002/adfm.202007226. (Visited on 12/16/2020).
- [23] Suganthan Veerachamy et al. "Bacterial adherence and biofilm formation on medical implants: A review". In: *Proceedings of the Institution of Mechanical Engineers, Part H: Journal of Engineering in Medicine* 228 (Oct. 2014), pp. 1083–1099. DOI: 10.1177/0954411914556137.
- [24] A. Gristina. "Biomaterial-centered infection: microbial adhesion versus tissue integration". In: *Science* 237 (Sept. 1987), pp. 1588–1595. DOI: 10.1126/science.3629258. (Visited on 04/06/2020).
- [25] Giampiero Pietrocola et al. "Colonization and Infection of Indwelling Medical Devices by *Staphylococcus aureus* with an Emphasis on Orthopedic Implants". In: *International Journal of Molecular Sciences* 23 (Jan. 2022), p. 5958. DOI: 10.3390/ijms23115958. URL: <https://www.mdpi.com/1422-0067/23/11/5958> (visited on 09/17/2022).
- [26] Niels Høiby. "A short history of microbial biofilms and biofilm infections". In: *APMIS* 125 (Apr. 2017), pp. 272–275. DOI: 10.1111/apm.12686. URL: <https://www.onlinelibrary.wiley.com/doi/10.1111/apm.12686>.
- [27] J. W. Costerton. "Bacterial Biofilms: A Common Cause of Persistent Infections". In: *Science* 284 (May 1999), pp. 1318–1322. DOI: 10.1126/science.284.5418.1318. (Visited on 08/21/2019).
- [28] Eve Maunders and Martin Welch. "Matrix exopolysaccharides; the sticky side of biofilm formation". In: *FEMS Microbiology Letters* 364 (June 2017). DOI: 10.1093/femsle/fnx120.
- [29] D Pavithra and Mukesh Doble. "Biofilm formation, bacterial adhesion and host response on polymeric implants—issues and prevention". In: *Biomedical Materials* 3 (Aug. 2008), p. 034003. DOI: 10.1088/1748-6041/3/3/034003.
- [30] D. Mack et al. "The intercellular adhesin involved in biofilm accumulation of *Staphylococcus epidermidis* is a linear beta-1,6-linked glucosaminoglycan: purification and structural analysis." In: *Journal of Bacteriology* 178 (Jan. 1996), pp. 175–183. DOI: 10.1128/jb.178.1.175-183.1996. URL: <https://jb.asm.org/content/178/1/175>.
- [31] Veronica Lazăr and Mariana Carmen Chifiriuc. "Medical significance and new therapeutical strategies for biofilm associated infections". In: *PubMed* 69 (July 2010), pp. 125–138.
- [32] Mira Okshevsky and Rikke Louise Meyer. "The role of extracellular DNA in the establishment, maintenance and perpetuation of bacterial biofilms". In: *Critical Reviews in Microbiology* 41 (Dec. 2013), pp. 341–352. DOI: 10.3109/1040841x.2013.841639. (Visited on 07/03/2020).
- [33] Brian P. Conlon. "Staphylococcus aureus chronic and relapsing infections: Evidence of a role for persister cells". In: *BioEssays* 36 (Aug. 2014), pp. 991–996. DOI: 10.1002/bies.201400080.

- [34] J.J.T.M. Swartjes et al. "Current Developments in Antimicrobial Surface Coatings for Biomedical Applications". In: *Current Medicinal Chemistry* 22 (June 2015), pp. 2116–2129. DOI: 10.2174/0929867321666140916121355.
- [35] Hossein Yazdani Ahmadabadi, Kai Yu, and Jayachandran N. Kizhakkedathu. "Surface modification approaches for prevention of implant associated infections". In: *Colloids and Surfaces B: Biointerfaces* 193 (Sept. 2020), p. 111116. DOI: 10.1016/j.colsurfb.2020.111116. (Visited on 04/04/2023).
- [36] H. Chouirfa et al. "Review of titanium surface modification techniques and coatings for antibacterial applications". In: *Acta Biomaterialia* 83 (Jan. 2019), pp. 37–54. DOI: 10.1016/j.actbio.2018.10.036. URL: <https://hal.archives-ouvertes.fr/hal-02397593/document>.
- [37] James B. Doub. "Bacteriophage Therapy for Clinical Biofilm Infections: Parameters That Influence Treatment Protocols and Current Treatment Approaches". In: *Antibiotics* 9 (Nov. 2020), p. 799. DOI: 10.3390/antibiotics9110799. (Visited on 11/15/2020).
- [38] Anjali Warriar et al. "Photodynamic therapy to control microbial biofilms". In: *Photodiagnosis and Photodynamic Therapy* 33 (Mar. 2021), p. 102090. DOI: 10.1016/j.pdpdt.2020.102090. URL: <https://www.sciencedirect.com/science/article/pii/S1572100020304440> (visited on 03/15/2022).
- [39] Eric J Hall and Amato J Giaccia. *Radiobiology for the radiologist*. 3rd ed. Wolters Kluwer, 2019, pp. 161–177.
- [40] Murat Beyzadeoglu, Gokhan Ozyigit, and Ugur Selek. *Radiation Oncology*. Springer Science Business Media, Apr. 2012.
- [41] Sarah Baatout. *Radiobiology Textbook*. Springer Nature, Sept. 2023, pp. 25–82.
- [42] Geou-Yarh Liou and Peter Storz. "Reactive oxygen species in cancer". In: *Free Radical Research* 44 (Jan. 2010), pp. 479–496. DOI: 10.3109/10715761003667554. URL: <https://www.ncbi.nlm.nih.gov/pmc/articles/PMC3880197/>.
- [43] Young-Seung Kim and Martin W. Brechbiel. "An overview of targeted alpha therapy". In: *Tumor Biology* 33 (Dec. 2011), pp. 573–590. DOI: 10.1007/s13277-011-0286-y.
- [44] Francisco D.C. Guerra Liberal et al. "Targeted Alpha Therapy: Current Clinical Applications". In: *Cancer Biotherapy and Radiopharmaceuticals* 35 (Aug. 2020), pp. 404–417. DOI: 10.1089/cbr.2020.3576.
- [45] Bryce J. B. Nelson, Jan D. Andersson, and Frank Wuest. "Targeted Alpha Therapy: Progress in Radionuclide Production, Radiochemistry, and Applications". In: *Pharmaceutics* 13 (Dec. 2020), p. 49. DOI: 10.3390/pharmaceutics13010049. URL: <https://pubmed.ncbi.nlm.nih.gov/33396374/>.
- [46] Robin M. de Kruijff, Hubert T. Wolterbeek, and Antonia G. Denkova. "A Critical Review of Alpha Radionuclide Therapy—How to Deal with Recoiling Daughters?" In: *Pharmaceutics* 8 (June 2015), pp. 321–336. DOI: 10.3390/ph8020321. URL: <https://www.ncbi.nlm.nih.gov/pmc/articles/PMC4491664/> (visited on 02/13/2020).
- [47] Muath Helal and Ekaterina Dadachova. "Radioimmunotherapy as a Novel Approach in HIV, Bacterial, and Fungal Infectious Diseases". In: *Cancer Biotherapy and Radiopharmaceuticals* 33 (Oct. 2018), pp. 330–335. DOI: 10.1089/cbr.2018.2481. URL: <https://www.ncbi.nlm.nih.gov/pmc/articles/PMC6207155/>.
- [48] B. van Dijk et al. "Treating infections with ionizing radiation: a historical perspective and emerging techniques". In: *Antimicrobial Resistance Infection Control* 9 (July 2020). DOI: 10.1186/s13756-020-00775-w.
- [49] E. Dadachova et al. "Feasibility of Radioimmunotherapy of Experimental Pneumococcal Infection". In: *Antimicrobial Agents and Chemotherapy* 48 (May 2004), pp. 1624–1629. DOI: 10.1128/aac.48.5.1624-1629.2004. (Visited on 09/02/2020).
- [50] Johanna Rivera et al. "Radiolabeled Antibodies to *Bacillus anthracis* Toxins Are Bactericidal and Partially Therapeutic in Experimental Murine Anthrax". In: *Antimicrobial Agents and Chemotherapy* 53 (Nov. 2009), pp. 4860–4868. DOI: 10.1128/aac.01269-08. (Visited on 03/13/2024).

- [51] B. van Dijk et al. "Radioimmunotherapy of methicillin-resistant *Staphylococcus aureus* in planktonic state and biofilms". In: *PLoS ONE* 15 (May 2020), e0233086–e0233086. DOI: 10.1371/journal.pone.0233086. (Visited on 10/15/2024).
- [52] Bruce van Dijk et al. "Evaluating the Targeting of a *Staphylococcus-aureus*-Infected Implant with a Radiolabeled Antibody In Vivo". In: *International Journal of Molecular Sciences* 24 (Feb. 2023), p. 4374. DOI: 10.3390/ijms24054374. URL: <https://pubmed.ncbi.nlm.nih.gov/36901805/> (visited on 06/30/2024).
- [53] Ekaterina Dadachova and Drauzio E N Rangel. "Recent Advancements in Radiopharmaceuticals for Infection Imaging". In: *Methods in molecular biology* 2813 (Jan. 2024), pp. 205–217. DOI: 10.1007/978-1-0716-3890-3_14. (Visited on 10/16/2024).
- [54] Emmanuel Deshayes et al. "Radium 223 dichloride for prostate cancer treatment". In: *Drug Design, Development and Therapy* 11 (Sept. 2017), pp. 2643–2651. DOI: 10.2147/DDDT.S122417. URL: <https://www.ncbi.nlm.nih.gov/pmc/articles/PMC5593411/>.
- [55] Robert Coleman et al. "A phase IIa, nonrandomized study of radium-223 dichloride in advanced breast cancer patients with bone-dominant disease". In: *Breast Cancer Research and Treatment* 145 (Apr. 2014), pp. 411–418. DOI: 10.1007/s10549-014-2939-1.
- [56] Sigma Aldrich. "Brain Heart Infusion Broth". In: *Merck* 1 (2024). URL: <https://www.sigmaaldrich.com/NL/en/product/sial/53286#product-documentation>.
- [57] Sigma Aldrich. "Brain Heart Infusion Agar". In: *Merck* 1 (2024). URL: <https://www.sigmaaldrich.com/NL/en/product/sial/70138>.
- [58] . *PALACOS LV+G – Low-Viscosity Bone Cement with Gentamicin*. Heraeus-medical.com, 2014. URL: <https://www.heraeus-medical.com/en/healthcare-professionals/products/palacos-lv-g/> (visited on 12/18/2024).
- [59] Hilbrand van De Belt et al. "Gentamicin release from polymethylmethacrylate bone cements and *Staphylococcus aureus* biofilm formation". In: *Acta Orthopaedica Scandinavica* 71 (Jan. 2000), pp. 625–629. DOI: 10.1080/000164700317362280. (Visited on 10/25/2019).
- [60] Daniëlle Neut et al. "Gentamicin release from commercially-available gentamicin-loaded PMMA bone cements in a prosthesis-related interfacial gap model and their antibacterial efficacy". In: *BMC Musculoskeletal Disorders* 11 (Nov. 2010). DOI: 10.1186/1471-2474-11-258. (Visited on 03/01/2023).
- [61] L. Pibida et al. "Determination of photon emission probabilities for the main gamma-rays of ²²³Ra in equilibrium with its progeny". In: *Applied Radiation and Isotopes* 101 (Mar. 2015), pp. 15–19. DOI: 10.1016/j.apradiso.2015.03.011. (Visited on 01/13/2025).
- [62] B.S Santos et al. "Spectroscopy and non-radiative processes in Gd³⁺, Eu³⁺ and Tb³⁺ tropolonates". In: *Spectrochimica Acta Part A Molecular and Biomolecular Spectroscopy* 54 (Nov. 1998), pp. 2237–2245. DOI: 10.1016/s1386-1425(98)00143-7. (Visited on 01/13/2025).
- [63] Nobuo Fukuda. "Apparent diameter and cell density of yeast strains with different ploidy". In: *Scientific Reports* 13 (Jan. 2023), p. 1513. DOI: 10.1038/s41598-023-28800-z. URL: <https://www.nature.com/articles/s41598-023-28800-z>.
- [64] . *How to optimise OD600 measurements*. www.bmglabtech.com. URL: <https://www.bmglabtech.com/en/howto-notes/how-to-optimise-od600-measurements/> (visited on 01/10/2025).
- [65] Michael Chavez, Jonathan Ho, and Cheemeng Tan. "Reproducibility of High-Throughput Plate-Reader Experiments in Synthetic Biology". In: *ACS Synthetic Biology* 6 (Nov. 2016), pp. 375–380. DOI: 10.1021/acssynbio.6b00198. (Visited on 02/05/2021).
- [66] João M. Monteiro et al. "Cell shape dynamics during the staphylococcal cell cycle". In: *Nature Communications* 6 (Aug. 2015). DOI: 10.1038/ncomms9055.
- [67] Portia Mira, Pamela Yeh, and Barry G. Hall. "Estimating microbial population data from optical density". In: *PLOS ONE* 17 (Oct. 2022). Ed. by Abdelwahab Omri, e0276040. DOI: 10.1371/journal.pone.0276040. URL: <https://www.ncbi.nlm.nih.gov/pmc/articles/PMC9562214/>.

A

Appendix A

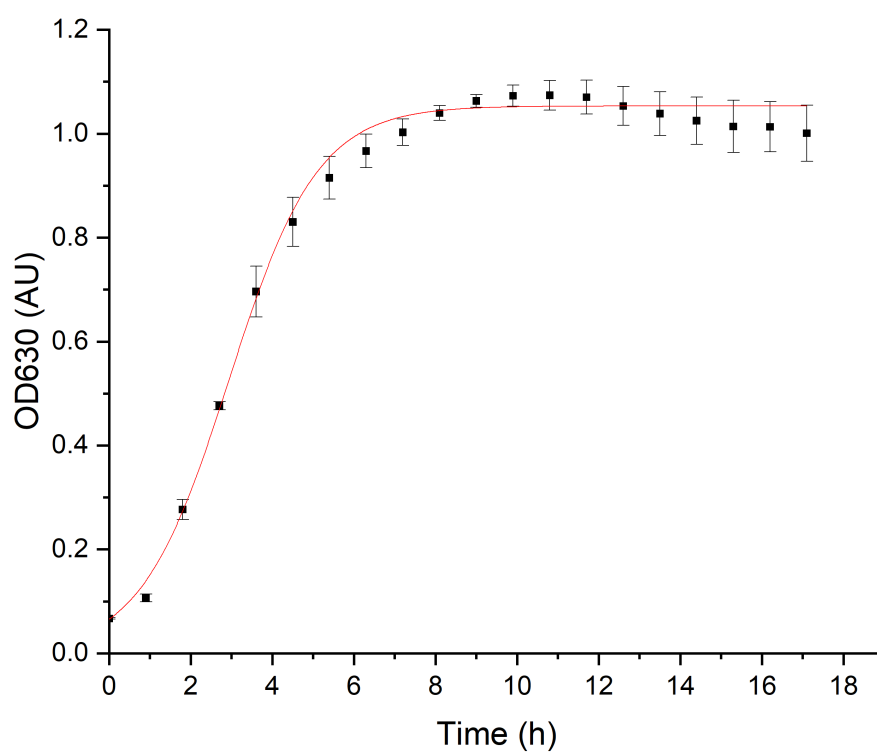


Figure A.1: Growth curve of *S. aureus* in BHI broth obtained through OD630 measurements during incubation at 37°C and low-shake for 18 h in a well-plate reader. Data points are an average obtained from six individual wells. Error bars represent their standard deviation.

This graph visualizes all data points from the growth of *S. aureus* without removing faulty measurements.

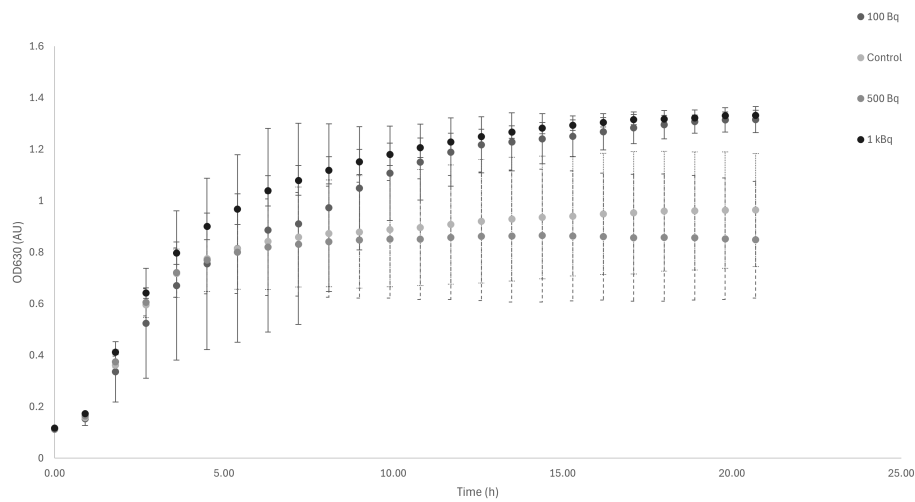


Figure A.2: Growth curves of *S. aureus* under different activities of radium-223 and the well plate covered with a Plate Sealer, obtained by OD630 measurements and incubation time of 21 h. The four growth curves are obtained from a single well-plate with each row of wells containing a separate activity. Error bars represent standard deviation of 6 separate experiments.

Growth curves obtained from the Ra-223 uptake experiment.

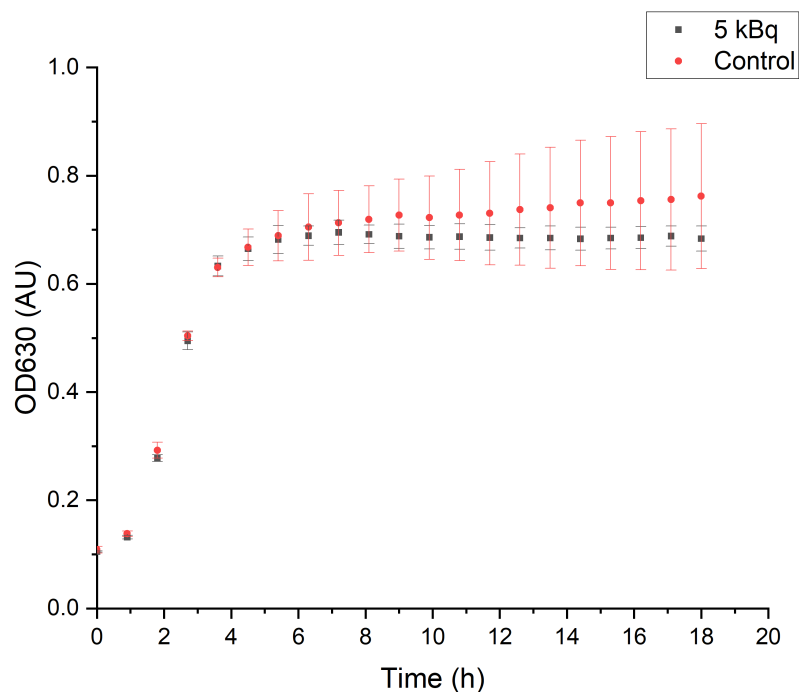


Figure A.3: Growth curves of *S. aureus* in presence of Ra-223 and the well plate covered with a Plate Sealer, obtained by OD630 measurements and incubation time of 18 h. The two growth curves are obtained from a single well-plate with each row of wells containing a separate activity. Error bars represent standard deviation of 5 separate experiments.